Ecological Indicators 71 (2016) 449–466

Contents lists available at ScienceDirect

Ecological Indicators

journal homepage: www.elsevier.com/locate/ecolind

A geospatial approach to monitoring impervious surfaces in watersheds using Landsat data (the Mondego Basin, Portugal as a case study)

Vasco M. Mantas [a,c,*], João Carlos Marques [b], Alcides J.S.C. Pereira [c]

[a] MARE – Marine and Environmental Sciences Centre, DCT, University of Coimbra, Portugal
[b] MARE – Marine and Environmental Research Centre, DCV, University of Coimbra, Portugal
[c] CEMUC – Department of Earth Sciences, University of Coimbra, Portugal

ARTICLE INFO

Article history:
Received 29 July 2015
Received in revised form 6 July 2016
Accepted 12 July 2016

Keywords:
Land use and land cover
Imperviousness
Environmental monitoring
Landsat
Watersheds

ABSTRACT

The urbanization of watersheds is a highly dynamic global phenomenon that must be monitored. With consequences for the environment, the population, and the economy, accurate products at adequate spatial and temporal resolutions are required and demanded by the science community and stakeholders alike. To address these needs, a new Impervious Surface Area (ISA) product was created for a Portuguese Watershed (Mondego river) from Landsat data (a combination of leaf-on multispectral bands, derived products, and NDVI time series), using Regression Tree Models (RTM). The product provides 30-m spatial resolution ISA estimates (0–100%) with a Mean Average Error (MAE) of 1.6% and Root Mean Square Error (RMSE) of 5.5%.

A strategy to update the baseline product was tested in earlier imagery (2001 and 2007) for a subset of the watershed. Instead of updating the baseline product, the strategy seeks to identify stable training samples and remove those where change was detected in a time series of Change Vector Analysis (CVA). The stable samples were then used to create new ISA models using RTM. The updated maps were similar to the original product in terms of accuracy metrics (MAE: 2001: 2.6%; 2007:3.6%).

The products and methodology offer a new perspective on the urban development of the watershed, at a scale previously unavailable. It can also be replicated elsewhere at a low cost, leveraging the growing Landsat data archive, and provide timely information on relevant land cover metrics to the scientific community and stakeholders.

1. Introduction

More than half of the world's population inhabits urban areas (U.N., 2014). In Europe, this figure is even higher, with 75% of the population (80% by 2020) living in cities (EEA, 2006). A similar urbanization trend was observed in Portugal in recent decades, where the urban population now reaches 42% of the total (INE, 2014).

In fact, urbanization is a global phenomenon that affects ecosystems, climate and the livelihood of human communities. In the United States alone, from 1982 to 2010, 17 million hectares of non-federal land were developed (USDA, 2013) and in Germany, 100 ha of land are transformed into built-up/transportation classes every day (DESTATIS, 2007). The overwhelming pace of urbanization in the second half of the 20th century changed the face of European cities, with the emergence of 'sprawling' phenomena and profound transformations in the overall urban growth patterns (EEA, 2006).

This seemingly irreversible trend is not always accompanied by the development of efficient urban planning policies that could emerge from modern science and technology (Marinoni et al., 2013). Therefore, it is urgent to develop environmental indicators that can be employed routinely in the monitoring of urbanized ecosystems on a regional and global scale and at a rate consistent with that of development (Tiner, 2004). These rapid mutations of the landscape led to a profound change in the science of urban ecology (Pickett et al., 2008), which became increasingly integrated, with contributions from ecology, physical, social, and economic sciences (Grimm et al., 2000). This "human-environment system" calls for new perspectives (Turner et al., 2007), to foster the development of original management policies focused on sustainability, while

* Corresponding author at: MARE – Marine and Environmental Sciences Centre, DCT, University of Coimbra, Portugal.
E-mail address: vasco_mantas@yahoo.com (V.M. Mantas).

http://dx.doi.org/10.1016/j.ecolind.2016.07.013
1470-160X/

accommodating growth and the population's legitimate aspirations (Marques et al., 2009).

Land Use and Land Cover (LULC) dynamics translate an otherwise abstract concept of change into measurable metrics, which can be objectively monitored to assess the impact over the health of land and aquatic ecosystems, the climate, and the territory (Loveland et al., 2002; Grove and Burch Jr., 1997). However such monitoring is not without challenges, as the urban and peri-urban space is inherently complex and highly heterogeneous, truly a patchwork of multiple LULC classes (Xian, 2008a,b; Bauer et al., 2008; Andrieu and Chocat, 2004). This complexity is the source of a multidimensional reality, with direct and indirect impacts over multiple biotic and abiotic variables, which may then influence social dynamics and interactions.

Stream hydrology and function are especially vulnerable to LULC (Morisawa Marie and Ernest LaFlure, 1979) and the concept of 'urban stream syndrome' was devised to describe the set of changes associated to streams draining developed lands (Walsh et al., 2005). Streams in urbanized catchments are characterized by channel instability (Bledsoe and Watson, 2001), changes in the volume and duration of surface runoff (Weng, 2001), channel incision, loss of large wood and sediment load (Vietz et al., 2014). Furthermore, the increased input of pharmaceuticals (Veach and Bernot, 2011), change in the nutrient load (Carey et al., 2013; Marinoni et al., 2013) and nonpoint-source pollution (Hurd and Civco, 2004; Brabec et al., 2002), or the change in sediment respiration rate (Feio et al., 2010) and in the benthic macroinvertebrate communities (del Arco et al., 2012) can also be attributed to urbanization and imperviousness. In fact, urban riparian areas can lose the ability to act as nitrate sinks (Groffman et al., 2003) or even foster nitrification (Pickett et al., 2008).

Land development is thus tied to an intricate, complex web of stressors that are hard to replicate in a controlled setting and are specific to each water body (Feio et al., 2010).

Adding to the aforementioned effects of imperviousness, the urbanization of watersheds has been suggested to influence litter breakdown rates and species richness. This relation can be explained by the increased flow of watersheds with higher levels of imperviousness, which may promote the physical degradation of litter (Chadwick et al., 2006; Paul et al., 2006). In fact several papers address the impact of imperviousness over invertebrate and fish populations (e.g. Chadwick et al., 2006; Roy et al., 2003; Miltner and White, 2004; Klein, 1979), vegetation structure and health (White and Grier, 2006; Song et al., 2015), and bird populations, which are negatively associated to the presence of paved surfaces (McClure et al., 2015).

However, the impact of urbanization goes beyond the deterioration of water quality, and it is directly connected to a decrease in the distribution and fragmentation of natural vegetation. In turn, the new urban environment influences the thermal conditions, originating the Surface Urban Heat Island (SUHI) (Yuan and Bauer, 2007; Xian, 2008b) even in shrinking cities (Emmanuel and Krüger, 2012). The SUHI consists in the increase of the surface temperature, observed in urban areas and that is strongly connected to the type of development and materials used (e.g. asphalt, rooftops) (Stathopoulou and Cartalis, 2007). The SUHI is the result of an accumulation of a significant amount of thermal energy, which may, in turn, generate a "thermal runoff response" (Kim et al., 2008) adding thermal pollution to the plethora of aforementioned stressors.

Interestingly, and despite the increasing global urban population, wide swaths of Europe and North America are subject to widespread shrinkage phenomena (Panagopoulos and Barreira, 2013). In the case of Portugal, by 2060, the population is projected to fall to 8.6 million, from the current 10 million (INE, 2014). In parallel, and even prior to the country's population decline, changes at the city level led to the relocation of the inhabitants to peripheral communities. Portuguese municipalities tend to react to the decline through investment, especially when the decline is associated to the young population (Panagopoulos and Barreira, 2013), which means that urbanization may not decline on par with population, but instead accelerate. This means that over the long term, in Portugal and elsewhere, the existing (or growing) infrastructure will have to be supported by a smaller population. This is thus a moment of particular importance in Europe, where the development of integrated monitoring strategies dedicated to developed lands takes center stage.

This reality is in contrast with that presented by many previous studies, which often focused on megacities (Duh et al., 2008; Grimm et al., 2008; Kraas, 2007) or regions of accelerated growth (Davis and Schaub, 2005) that may not be representative of the regional or even national realities within parts of continental Europe.

In face of the increasingly complex and challenging scenario, cities and communities are struggling to improve environmental standards through the establishment of urban sustainability goals (Duh et al., 2008). Information, namely regarding the sealed or impervious surfaces that characterize urban environments, becomes central to the development of such planning and mitigation strategies (Bauer et al., 2008; Young et al., 2013). This context of extremes is motivating an increased awareness to the fact that data users need timely land cover products capable of offering an accurate depiction of the urban environment (Xian and Homer, 2010). The widespread use of remote sensing and Geographic Information Technologies (GIT) opened a new chapter in the characterization of land cover trends, watershed planning, and modeling (Tiner, 2004; Brabec et al., 2002).

Ridd (1995) first described the Vegetation-Impervious-Soil (V-I-S) model as a possible answer to quantitatively describe the urban morphology and therefore fulfill the emerging promise of accurate land cover mapping brought by multispectral satellite imagery. In recent years, and especially after 2000, a growing number of studies addressing the use of remote sensing of developed lands have been published although significant challenges persist (Weng, 2012).

Yang et al. (2003) describe the "anthropogenic impervious surface" as an indicator of the spatial extent and intensity of urban development. Rooftops, roads, sidewalks, and compacted soil constitute examples of impervious surfaces (Arnold and Gibbons, 1996), which are ecologically important because of their nature and arrangement (Schwarz, 2010). The Impervious Surface Area (ISA) – the impervious fraction within a pixel – can thus become the "self-consistent metric" enabling accurate comparative analysis of urban extents in transboundary regions (Xian, 2008a,b).

Categorical classification systems (e.g. Anderson et al., 1976) can at times create artificial dichotomies between natural and developed lands, ignoring the continuum best described by pragmatic metrics that can be used in interdisciplinary studies (Cadenasso et al., 2007; Arnold and Gibbons, 1996). ISA does not describe function but only the amount of artificialization, which can be the driving force behind stream degradation and nonpoint-source pollution (Slonecker et al., 2001) at thresholds as low as 10% (Arnold and Gibbons, 1996). Although several authors suggest this threshold as key for stream degradation, permanent changes can be detected earlier, depending on the geographic context and parameter in analysis (Vietz et al., 2014; Chin, 2006; Bledsoe and Watson 2001).

Previous studies addressed the problem of ISA mapping using different or adapted strategies, sometimes relying in significant generalizations (Esch et al., 2009). Data sources range from optical sensors, RADAR, and LiDAR and techniques include Regression Analysis (Sexton et al., 2013; Bauer et al., 2008; Hodgson et al., 2003), Classification and Regression Trees (CART) (Jiang et al., 2009), Spectral Mixture Analysis (Li et al., 2015; Zhang et al., 2014a,b,c; Wu, 2004; Yuan and Bauer, 2007), Hyperspectral data

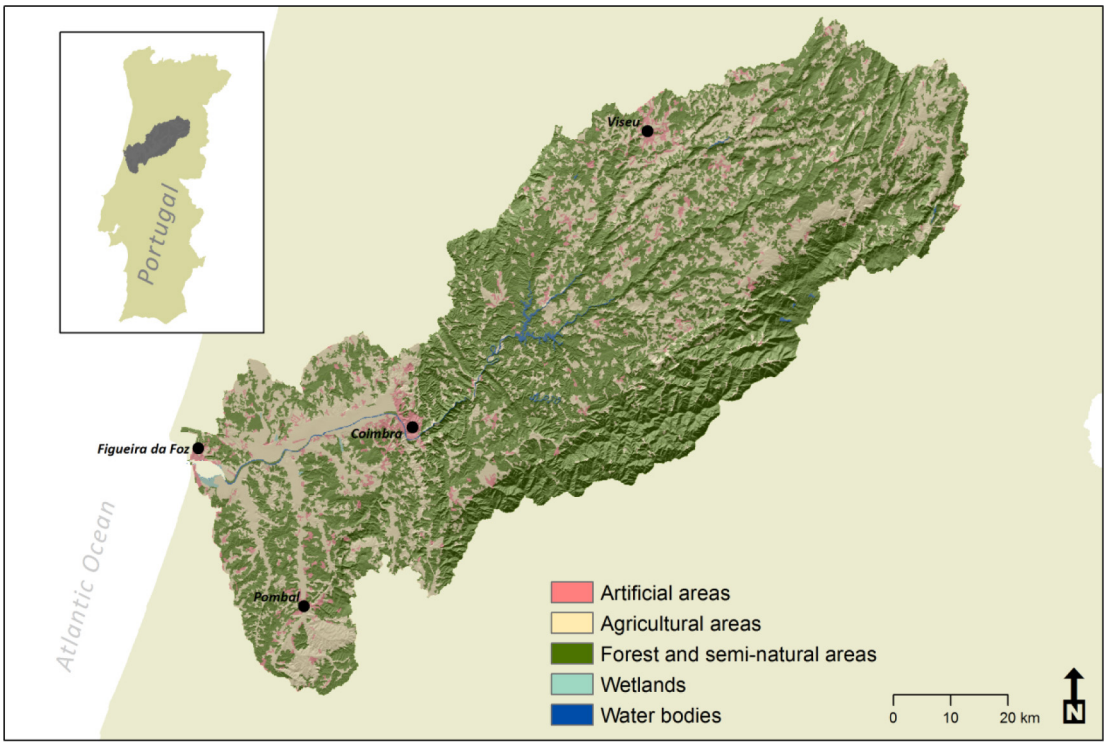

Fig. 1. Map of the Mondego river Watershed, depicting a simplified land cover map (CORINE, 2016), location of major urban centers, and terrain.

analysis (Van der Linden and Hostert, 2009), Maximum Likelihood Classification (Jia et al., 2014), Multivariate Texture (Zhang et al., 2014b), and onscreen interpretation (Loveland et al., 2002). We suggest Weng (2012) for a comprehensive review of recent and historical methods used for ISA mapping.

Model performance is a function not only of the methodology but also of internal heterogeneity of the target area (Parece and Campbell, 2013). Thus, the comparison of methodologies relying on multispectral data, including regression modeling, regression trees, and SMA is often site-specific, but performance differences are frequently negligible (Yuan et al., 2008). Hyperspectral data, on the other hand, promises to meet the spectral requirements of urban mapping (Herold et al., 2003), but the lack of systematic and affordable data limited the employment of these datasets in systematic mapping programs. Combining Synthetic Aperture Radar (SAR) and optical data may improve imperviousness estimates in all-weather conditions, through the reduction of the uncertainty associated with bare soil, shaded areas, and water surfaces (Zhang et al., 2014a,b,c). Sentinel-1, a SAR-equipped satellite of the European Space Agency (ESA) is likely to give an important contribution to accelerating research on this topic, considering the high spatial and temporal resolution as well as the open access policy. This is particularly important considering that the use of a single SAR image yields poorer results when compared with the equivalent use of a unique Landsat scene (Zhang et al., 2012).

High-resolution imagery can broaden the perspectives on urban mapping and interpretation, namely through the use of image segmentation techniques (Thomas et al., 2003). However, data costs are still prohibitive for regional or national mapping initiatives, especially when unsupported by government agencies or sizeable private companies. Previous studies often stress the relevance of data accessibility and spatial resolution in the data selection process. The necessary compromise between technical requirements and cost fostered the adoption of multispectral optical data as the preferred source of information (Deguchi and Sugio, 1994). Landsat, in particular, offers several advantages to these studies, including the long-term digital archive, adequate spatial and spectral/radiometric resolution, and open data policy (Goward et al., 2006; Yang et al., 2003).

Because urban landscapes are highly heterogeneous, and most pixels composed of a mixture of different surfaces with different spectral properties (Wu, 2004), subpixel analysis is needed to quantify the contribution of each component to the overall structure (Yang et al., 2003; Xian, 2008a,b). Therefore, ISA, as a continuous variable, avoids the problems inherent to nominal classes, which is particularly relevant within the urban and peri-urban matrix (Bauer et al., 2008). The spatial resolution of current Landsat sensors is particularly suited to pursue this goal. A comparison with coarser products (e.g. CORINE, 2016; Fig. 1) emphasizes the importance of accurately depicting the connectivity of artificial surfaces and measure relevant metrics at the sub-pixel level. The spectral mixture of complex, large pixels in urban and peri-urban landscapes hampers the accurate retrieval of land cover metrics and impedes the depiction of the continuous urbanization gradient.

As aforementioned, the importance of monitoring urbanization derives in part of the rapid evolution of urbanized regions worldwide. However most land cover products are published several years after the original image acquisition, and are therefore outdated when published (Xian and Homer, 2010). It is therefore necessary to provide stakeholders and managers with high temporal resolution products focused on urban development, which requires a significant effort into the development of updating strategies (Jin et al., 2013; Weng, 2012; Sexton et al., 2013; Jensen and Cowen, 1999).

Existing strategies used to update ISA maps differ, but often require some level of prior knowledge on land cover, the use of dense time series or of anniversary imagery, requirements that are not always easy – or possible – to fulfill (Jin et al., 2013; Jia et al., 2014; Xian; Huang et al., 2010).

A common trait to all visions is the requirement of high quality ground truth samples, which is one of the critical and most time consuming components of the process.

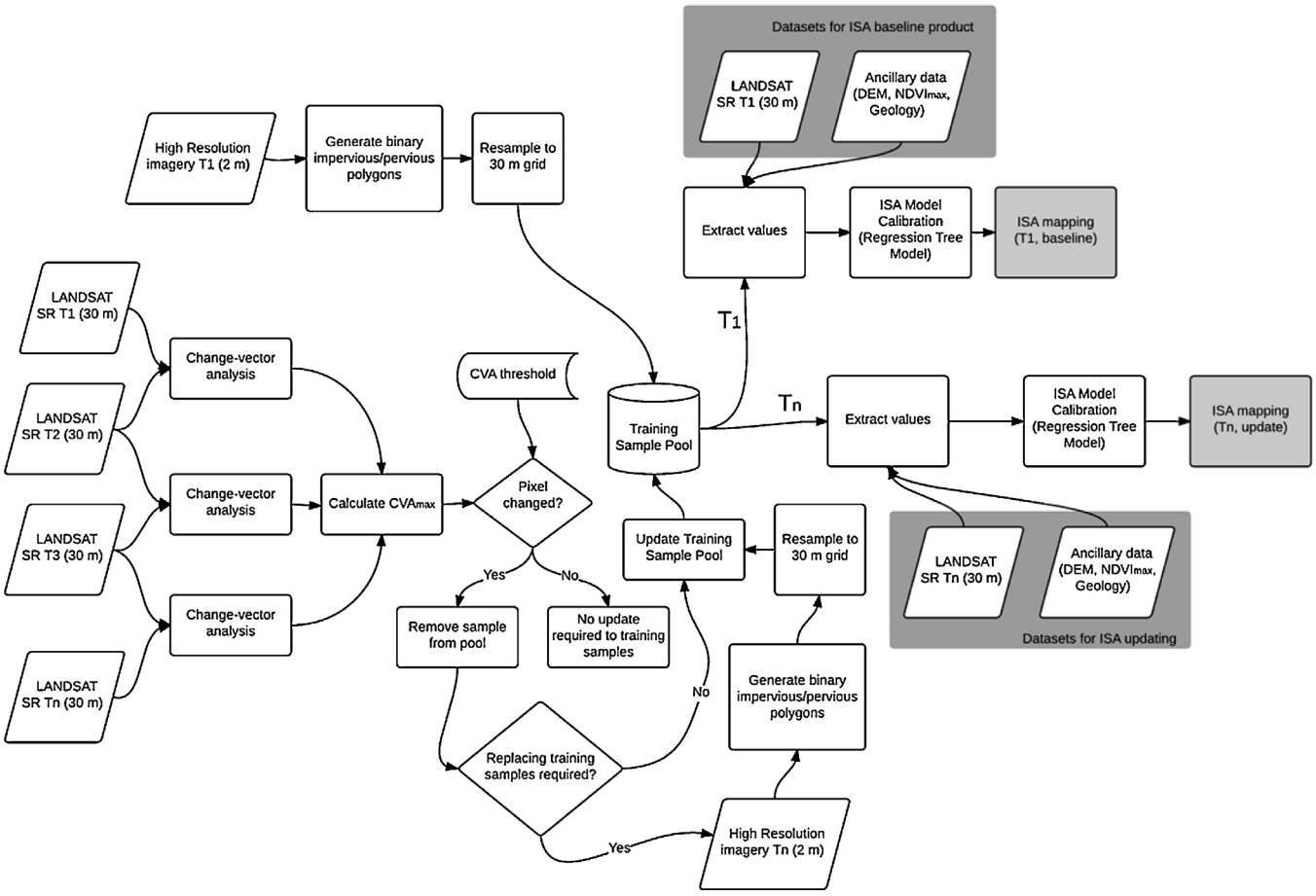

Fig. 2. Generalized workflow of the methodology employed to map Impervious Surface Area (ISA) using Landsat data, and subsequent updates through Change-Vector Analysis (CVA). Baseline product (T1) matches ISA2013 in this paper, while the update (at an earlier or later date) (Tn), corresponds to the ISA2001 and ISA2007 tests.

In Europe, a fast and cost-effective approach to ISA mapping is still missing (Esch et al., 2009). The CORINE Land Cover, a project of the European Union, partially fulfills this objective by providing cartography of European countries (39) using 44 thematic classes at spatial resolution of 100 and 250 m (CORINE, 2016). These products are often used in numerous studies and applications where land cover is relevant (Martínez-Fernández et al., 2015; Suau-Sanchez et al., 2014; Pilli, 2012; Teixeira et al., 2014), with urban classes being merged to represent the "sealed surfaces" (Schwarz, 2010). However, CORINE land cover database does not have the necessary thematic and spatial resolution for several critical hydrologic and watershed management applications (Macary et al., 2014) or biomass and carbon assessment studies in the urban context (Raciti et al., 2014).

The European Copernicus program also publishes five high resolution layers (HRLs) on land cover characteristics that can provide additional information on land cover, including imperviousness (Langanke et al., 2013). Validation of the Copernicus HRL is still ongoing and therefore it is difficult to ascertain the quality of the product in its current version. Data distribution of the Copernicus layers is subject to restrictions, limiting access to the information by the potential user community.

1.1. Research objectives

This study describes the development of an Impervious Surface Area (ISA) product for a baseline reference date of 2013 (ISA2013) covering the entire Mondego river Watershed, in Portugal (Fig. 1). Focusing the study in a watershed is a strategic decision that aims to avoid the dissection of an otherwise geographically coherent unit into multiple ecologically-irrelevant administrative regions (Grimm et al., 2000).

We also present a processing scheme for semi-automated updates and test the approach for two periods (2001 and 2007) in two representative and contiguous counties (Coimbra and Condeixa-a-Nova), characterized by heterogeneous LULC. The update strategy differs from other mapping initiatives because instead of identifying the changed pixels in the baseline ISA map, it searches for stable training samples. These samples are then used as independent variables in a regression tree model, together with new samples that replace the changed ones if necessary. We hypothesize that this strategy, 1) originates a more homogeneous pool of training samples that can be used across different dates and even as mapping methodologies evolve, 2) results in more homogeneous and comparable products, 3) updated ISA maps do not necessarily carry the errors of previous model runs. Finally, the advantages of a regional approach to imperviousness mapping are discussed along with plans for the operational distribution of the generated datasets in a platform designated as "Smart Basins".

2. Materials and methods

The methodology can be summarized as the following sequence (Fig. 2): a) acquire and pre-process remote sensing and ancillary data (section 2.2); b) create detailed samples of pervious/impervious surfaces through the visual interpretation of high resolution imagery (section 2.4); c) create the baseline Impervious Surface Area model for 2013 using Landsat and ancillary data

(section 2.5); d) characterize change in a subset of the study area (section 2.6); e) update high resolution samples (created in b)), through the removal of the changed areas from the pool using a method based on annual time series of Change Vector Analysis (section 2.6); f) update the ISA models (2001 and 2007) using the updated training sample database (section 2.6).

2.1. Study area

The Mondego river is the largest under exclusive Portuguese administration (Fig. 1) with a basin covering 6670 km^2. The watershed is often divided into three different regions including the estuary, the "Lower Valley" (to the West) and the "Upper Valley" (to the East) (e.g. Teixeira et al., 2014).

The "Upper Valley" is characterized by topographically complex terrain where the headwater is located ("Serra da Estrela", with a maximum elevation of 1993 m). This area is geologically dominated by igneous (granites) and metamorphic rocks (mainly schist and graywackes). The western sector of the basin ("Lower Valley") is characterized by gentle slopes and mild elevations with sedimentary rocks (mostly sandstones and limestones) of Mesozoic and later ages, often supporting valuable farmland along the flat floodplains. The river meets the Atlantic Ocean in a small mesotidal estuary, subject to strong anthropogenic pressure (Marques et al., 2002; Cunha and Dinis, 2002). Agricultural, industrial, and other human activities upstream are responsible for frequent eutrophication episodes (Marques et al., 2003).

The basin is home to an estimated permanent population of 712969 (ARH, 2012) in 46 counties. The most significant urban centers (counties) are Coimbra (138 058 inhabitants in 2013), Viseu (98 601), Figueira da Foz (61 291), and Pombal (54 413) (INE, 2014). Central Portugal, a statistical unit that comprises the Mondego river Watershed is subject to a significant population decline, having lost 58 111 inhabitants between 2001 and 2013 (INE, 2015)

According to the CORINE 2012 land cover product, only 3.3% of the watershed is occupied by artificial areas (Fig. 1). Forest and semi-natural areas (64.3%) and agricultural uses (31.8%) occupy the bulk of the surface cover across the basin. Geology and topography control the distribution of these classes, which are, nonetheless, found evenly interspersed in the watershed.

The socio-economic relevance of the territory supports the integration of the imperviousness products with the human dimensions of the basin, in support of the development of a future, integrated, data analysis platform.

2.2. Remote sensing datasets

Remote sensing data were used to generate the training samples (used as 'ground truth') and as the main input to the ISA model and change detection protocol. The delineation of the training samples followed a protocol based on the visual interpretation of high resolution satellite and aerial imagery, while the ISA models were built using Landsat data. Both protocols are described in the following sections.

Three different high resolution data sources were used as 'ground truth' across the different steps of the workflow. Notice that the high resolution imagery was not employed directly in the implementation of the ISA model, but only as the source of information for the delineation of training samples and validation of the methodologies.

For the *circa* 2001 coverage, we obtained aerial photographs in natural color mode acquired by the *Instituto Nacional de Intervenção e Garantia Agrícola* (an Institute of the Portuguese Ministry of Agriculture) in the year 2000. The images are provided as orthophotomaps with a spatial resolution of 0.5 or 1m, depending on the geographic area. In this study samples from both collections were used.

For the 2007 regional ISA model, we relied on aerial photographs acquired by the Portuguese Geographic Institute (IGEO) in the same year. The mosaics are distributed as 'true color' orthophotomaps with a spatial resolution of 0.5 m. Finally, the calibration and validation of 'ground truth' datasets for the 2013 baseline ISA product were created using high resolution satellite imagery acquired in 2012 and 2013 from multiple sources including QuickBird 2 and WorldView 1/2. The data were accessed as 'true color' pan-sharpened, orthorectified images with a spatial resolution between 0.5 and 0.65 m depending on the sources.

All high resolution images were resampled to a common spatial resolution of 1 m to standardize mapping procedures across regions and dates, and allow a common Minimum Mapping Unit, as described in the following section. True color composites were used in the interpretation process, since it was the only band combination common to the datasets from all periods. The use of additional bands would have contributed to improve the delineation of the training samples, by reducing the uncertainty in the classification as pervious/impervious. However, in the absence of data with common spectral attributes, it was considered preferable to homogenize the data sources used for classification.

The development of the ISA model relied on the use of Landsat Surface Reflection (SR) products for both the baseline 2013 research-grade product and the 2001 and 2007 updating tests. For the 2013 product, all imagery was acquired by the Operational Land Imager (OLI) equipping Landsat-8. For both the 2001 and 2007 tests, a combination of TM and ETM+ data from Landsat-5 and 7 were used. Two scenes are required to map the entire watershed (Path 204 Row 032 and Path 203 Row 032).

Previous studies differ on the atmospheric correction methods (if any) employed to normalize the Landsat imagery. The Multi-Resolution Land Characteristics Consortium 2001 protocol (Chander et al., 2009) limits processing to at-sensor reflectance. This protocol is then used in by other authors (e.g. Xian et al., 2009; Homer et al., 2004; Jin et al., 2013; Yang et al., 2003; Wu, 2004). Other studies use more sophisticated atmospheric correction methods including the ATCOR2 algorithm (Esch et al., 2009) or 6 S (Sexton et al., 2013). Huang et al. (2010) reports there are little differences in the detection of disturbance and classification using Surface Reflectance (SR) and At-Sensor imagery.

Nonetheless, in this paper, because we used a long time series acquired by different sensors (Pacifici, 2014), we adopted a conservative approach, relying on SR data, made available by the United States Geological Survey for Landsat 4-5 TM, −7 ETM+ and −8 OLI (Masek et al., 2013; United States, 2015).

The imagery selection process included a visual inspection and the removal of scenes with cloud cover exceeding a pre-defined threshold of 8% for the relevant land area. The Quality Assessment band (QA) distributed with the Landsat SR product was relevant in this context by providing a simple and objective way to determine the usable area within the scene. The presence of dust and smoke, wildfires or haze was also considered in the quality assessment. For selected scenes, areas affected by clouds were filled by temporally close acquisitions (within 1 month of the target image).

Although a single image was used as reference for each product date (2013 and the 2001 and 2007 updates), a larger number of images were acquired for the extraction of ancillary data, including phenology information. We hypothesized that the fluctuations in the Normalized Difference Vegetation Index (NDVI) across a phenological cycle could improve the performance of the ISA model. Urban areas have generally stable and low NDVI values, whereas forests and semi-natural areas have higher NDVI amplitudes across the year and generally higher values. Cropland displays significant NDVI fluctuations across the growing season, which can be

captured in the time series. As such, the highest NDVI value was extracted for each reference year (per pixel) as well as the amplitude value, using the highest and lowest values within the $\mu \pm 2\sigma$ range, in order to minimize the impact of image artifacts. This expedite phenological characterization was based on 8 images for 2013, 15 images for 2007, and 6 images for 2001. The number of images used in 2007 reflects the need to compensate the localized data loss caused by Landsat-7's SLC-OFF malfunction. Missing values were not filled in this instance.

On the other hand, for change detection, and considering that we were interested in inter-annual change, one image was selected for each year between 2000 and 2013. The anniversary images were selected using as reference the baseline 2013 image used to build the ISA model (acquired in 2013/251). The SLC-OFF malfunction was addressed in this case, given that for the years 2004, 2005, 2008, 2009, and 2012 no alternate Landsat dataset was available. The missing values of the anniversary image were filled using same-season (summer) imagery acquired in the closest viable acquisition(s) of two preceding months. The replacement data were first histogram-stretched to reduce the phenological differences between both acquisitions, using the intact pixels as reference. It is also important to notice that the test areas, where the Change-Vector Analysis was applied are only marginally affected by the SLC-OFF problem, due to their location within the scene. With the increasing availability of Landsat-8 and Sentinel-2 data, the application of the method in the future should be streamlined.

The multispectral bands were used to compute several products including Principal Component Analysis (PCA), Normalized Difference Vegetation Index (NDVI), Normalized Burn Ratio (NBR), Normalized Difference Moisture Index (NDMI), and the ratios $B6.B7^{-1}$, $B5.B6^{-1}$ and $B4.B2^{-1}$ (band numbers relative to the Operational Land Imager).

2.3. Ancillary data

To support the development of the ISA models, ancillary data were used to provide context information, which may be relevant in the construction of the models and interpretation of results.

Topographic contour lines were extracted from the military maps of the watershed at a scale of 1:25 000 and used to build a 30 m Digital Elevation Model (DEM) collocated to the Landsat imagery. Slope maps (percentage), slope aspect (degree), Valley Depth and Dominant Landform rasters were generated from the original DEM using SAGA GIS. The watershed was also segmented into sub-basins, using automated stream delineation and catchment area calculation tools, available with the ArcHydro package for ArcGIS.

A simplified Geological Map at a scale of 1:100 000 was also used in the construction of the ISA models. The vector map was converted to cells, collocated to the Landsat imagery. Each cell was assigned to the dominant geological formation within the pixel area.

A land cover product distributed by the Portuguese government (COS2007) and produced from the interpretation of aerial photography, with a Minimum Mapping Unit of 1 ha (IGP, 2010) was used in support of change-vector analysis.

Census records were downloaded from the Portuguese Statistics Institute (INE) for the counties and parishes ("Freguesias") of the Mondego river Watershed.

Road and street data were downloaded from the Open Street Map website (OSM, 2015). To each road segment, attributes on speed limit and direction were added to the geodatabase. The street data were used to calculate average transit times (service areas) from central Coimbra, using the Network Analyst tool available in ArcGIS.

2.4. Training samples

The development of the ISA model (2013) requires the delineation of high spatial resolution training samples, which are used as ground truth in the ISA regression tree model. The samples were manually mapped by the authors upon interpretation of the high resolution satellite and aerial imagery. A common Minimum Mapping Unit of 4 m^2 was used in the delineation of pervious and impervious surfaces, which were stored as vectors in a geodatabase. Each contiguous mapping block covered a minimum area of 8100 m^2 (equivalent to 3×3 Landsat pixels), i.e. no smaller and disconnected samples were mapped.

The resulting binary (pervious/impervious) vector file was then converted to a regular grid with a spatial resolution of 30 m and collocated to the Landsat pixels. Each cell thus generated contains the percentage of pervious and impervious fraction within the pixel area. A total of 148 055 cells (covering 133.25 km^2) were created using this method and used in the calibration of the ISA regression tree model. An additional set covering 14 000 pixels (*ca.* 10% of the calibration set) was used to validate the model, using the same mapping methodology.

The samples are representative for different land cover classes and intra-class variability. Particular attention was given to different types of urban infrastructures and housing types to account for the wide range of materials and development intensities. Given the area of the watershed, and despite its internal diversity, no stratification of the AOI was made based on ecoregions or topography. Nonetheless, sample data were stratified by vegetation cover type to account for the seasonal variability in greenness between vegetative cover types (Bauer et al., 2008). The stratification resorted to the classes included in the CORINE 2012 land cover map. An equivalent number of sampling points were delineated for each class.

The method described in section 2.6, addresses the selection of the training samples thus created, from stable areas, for ISA product updates (in the study for the reference years of 2001 and 2007).

2.5. ISA regression tree model

Regression Tree Models (RTM) are machine-learning algorithms described in great detail by Breiman et al. (1984). RTM algorithms partition the original sample and create a tree that includes a combination of a descriptor and a linear regression (Yang et al., 2003; Xian, 2008a,b). The combination of all the rules and equations describe the sample used to recursively build the model, simplifying nonparametric and nonlinear relationships between the different variables. In the case of the ISA model, each linear regression enables the estimation of the percentage of impervious surface, per pixel, for a subset of the complete sample. The model relies on high quality training samples which are used as a continuous dependent (target) variable. The satellite imagery and other ancillary data (topography and geology) become the independent or explanatory variables during model development. The imagery used includes anniversary, leaf-on Landsat-8 OLI multispectral bands and derived products as well as a set of two rasters containing the Maximum and Minimum NDVI value for the hydrological year. The ISA2013 model was built on Weka using the M5 P algorithm (Quinlan, 1992) and translated into GeoTIFF rasters (one per rule) using a custom python script developed by the authors for ArcGIS. Each raster was then combined into a single image file containing the ISA estimates for the entire watershed. The product describes the imperviousness level of the Watershed, at a spatial resolution of 30 m and for the reference year of 2013.

The validation of the model outputs relied on traditional accuracy metrics (Janssen and van der, 1994) applied to independent reference data (equivalent to 10% of the calibration set). Amongst

the metrics used is the Mean Average Error (MAE), which is calculated as:

$$MAE = \frac{1}{n}\sum_{i=1}^{n}|ISA_m - ISA_g| \quad (1)$$

Where ISA_m is the estimated impervious surface area and ISA_g is the ground truth for the same pixel.

The Root Mean Square Error (RMSE) was also calculated for all outputs. The RMSE is calculated as:

$$RMSE = \sqrt{\frac{1}{n}\sum_{i=1}^{n}(ISA_m - ISA_g)^2} \quad (2)$$

The Pearson correlation coefficient was used to assess the linearity of the correlations between ISA estimates and ground truth data. The Pearson correlation coefficient (r) is calculated as follows:

$$r_{xy} = \frac{Cov(ISA_m Y)}{\sqrt{Var(ISA_m)}\sqrt{Var(Y)}} \quad (3)$$

where Y is the variable under study.

Univariate least squares regression analysis was used to determine the correlation between ISA2013 and census data. Analyses were conducted in several variables including population at county and parish ("freguesia") levels as well as county purchasing power (PP). For each variable, the hypothesis H_0: $\beta_1 = 0$, where β_1 is the model's slope parameter, was tested for a significance level of 1% at Microsoft Excel. Considering the mismatch between watershed limits and the administrative boundaries of counties and parishes, it was not possible to extend the analysis to the entire watershed. Instead, only counties in which 70% of the territory was located within the Mondego watershed and contained the most significant urban center were considered, totaling 24 municipalities. Of these, 10 counties were entirely located within the watershed and 10 had over 90% of the territory inside the study area. In the case of parishes, the smaller area simplified the process, and all jurisdictions entirely within the watershed were considered (n = 241). Taking into account the large sample it was deemed unnecessary to include parishes that spread across multiple watersheds, thus limiting the sources of error.

Using the ISA2013 dataset, the imperviousness of sub-basins found within the watershed was determined, in order to compare the estimated values with the 10% and 30% ISA thresholds suggested by Arnold and Gibbons (1996). The sub-basins were delineated from the regional Digital Elevation Model using ArcHydro (at ArcGIS). The minimum drainage area (flow accumulation) threshold required for stream and sub-watershed delineation were set to 10 000 pixels for a raster with a spatial resolution of 25 m. The ISA2013 was then calculated for each sub-basin using zonal statistics and compared with the predefined stream status thresholds.

2.6. Change detection and updates to the baseline product (ISA2013)

The development of high quality training data is one of the barriers preventing frequent updates to land cover maps (Yang et al., 2003). Therefore, previous studies discussed the advantages – and disadvantages – of manual photo interpretation against automated classification (Xian, 2008a,b) and strategies for sample selection (Jia et al., 2014).

One of the objectives of the study is to assess the feasibility of future near real-time updates to the baseline 2013 product (forward and backward analysis). Instead of updating the changed pixels in the ISA map, our methodology identifies the stable training samples and runs the model using this set. New samples can be created to replace the flagged ones as needed, in order to maintain the variability of ISA within the pool of training areas. For this purpose, a simple strategy was devised that relies on the construction of a time series of change, based on the analysis of anniversary multispectral Landsat Surface Reflectance data. To reduce the amount of change due to phenological differences, a maximum tolerance of 1 month from the reference date was allowed (Xian and Homer, 2010). The reference anniversary data were acquired over the summer to reduce the effect of topographical shadows. The test was conducted in the contiguous Coimbra and Condeixa-a-Nova Counties, which are characterized by a diverse land cover, terrain, and geology. Furthermore, the two counties display different population growth trajectories, with significant population movements from Coimbra to Condeixa. This fact poses interesting opportunities to study the influence of population dynamics over ISA.

Image pairs (yearly) were analyzed using the Change Vector Analysis (CVA) methodology (Malila, 1980) from the year 2000 up to 2013.

Change Vector Analysis magnitude is calculated as:

$$\rho = \sqrt{\sum_{n=1}^{6}(X_{n,r} - X_{n,s})^2} \quad (4)$$

where, the number of reflectance bands of Landsat is represented as n, X_r is the early date image and X_s the late date image. The CVA yields a change magnitude and it is through the comparison against a pre-defined or empirically derived threshold that change is detected and flagged. Average CVA magnitudes differ for different land cover classes and can be adjusted for automated change detection (Xian et al., 2009; Xian and Homer, 2010). However, in this study, no prior land cover information was available at the same scale and therefore a different approach was required.

After this initial step, the highest value in the time series is assigned to the pixel (CVA_{max}). The CVA_{max} can then be compared against a threshold to determine whether change occurred over the period. In summary, the CVA_{max} is calculated from all anniversary image pairs available from the date of the initial baseline product (not the last update) to the date of the new ISA map. The process can be applied both to earlier or later dates. The identification of an optimum threshold for change detection was made empirically as follows.

The Portuguese COS2007 land cover map was used to randomly create 400 points for each of the consolidated land cover classes (artificial, forest and semi-natural, agricultural areas, wetlands). For each point, the CVA_{max} was retrieved along with a change/no-change flag based on the interpretation of the 3 sets of high resolution imagery already described in section 2.2. Using the information thus acquired, a conservative (common) value was determined that enables the selection of unchanged areas across the different land cover types. The maximum CVA for the entire study period (CVA_{max}) admitted for a pixel to be considered as no-change and maintained in the pool of training samples matches the 2.5% lower values found within the watershed (or a CVA_{max} of 0.1 in the study area).

A training sample located in a pixel marked as changed is flagged in the database and is not used in subsequent product updates. It can, nonetheless, continue to be used in the reprocessing of earlier-date products, before change was signaled by the method.

This approach is only possible because we are not updating the cartographic products but removing the changed training samples used in the classification process. This may lead to an over extraction, which in this case is preferable over the use of erroneous inputs to the model. By updating the training samples and not the earlier-date product (i.e. as in the National Land Cover Database approach), it becomes possible to update the mapping methodologies as new

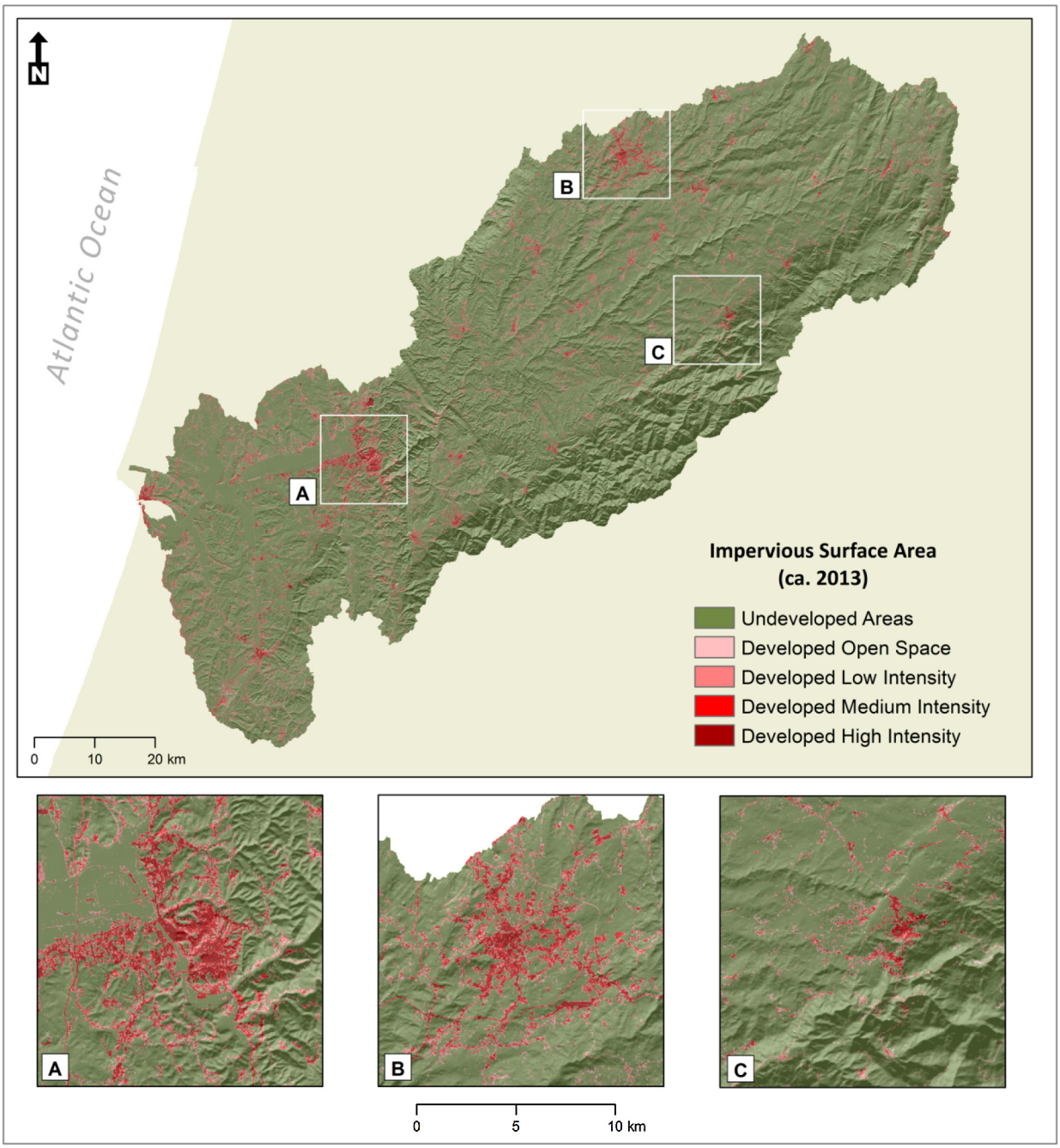

Fig. 3. The Mondego river Watershed Impervious Surface Area for *circa* 2013 (ISA2013). Three representative areas are displayed in greater detail including Coimbra (A), Viseu (B), and Seia (C). The ISA classes are described in the text.

sensors and methods become available, without creating hybrid cartographic products.

A confusion matrix was built to calculate the accuracy of the concept, using an additional independent set of 316 random points, which were visually analyzed for change detection using the three sets of high resolution imagery (2001, 2007 and 2013). The interpretation was then compared with the automated change detection protocol for validation purposes.

Upon validation, the methodology was applied to the 2013 baseline training sample described in section 2.4, to create products for 2001 and 2007. A subset of the complete pool of training samples (watershed-wide) was generated from the data located in the two test counties for the purpose of this test. The ISA2013 product was then reprocessed (herein named $ISA_{sub}2013$) using the training sample subset to guarantee comparability between the baseline subset and the updated products. The sample subset was then screened for change using the aforementioned CVA-based methodology and ISA products generated for 2001 and 2007, using the Regression Tree Model method described in section 2.5.

The three ISA datasets were analyzed in detail in the two test counties and changed pixels were extracted after identification using the aforementioned methods. The changed pixels were quantified and then characterized according to a three-class system, upon visual interpretation of the high resolution imagery. The categories considered included residential areas (e.g. apartment buildings and single-family housing), services (e.g. commercial areas, schools), and infra-structure (e.g. roads, parking lots). These metrics were calculated for the subsetted test area, individual coun-

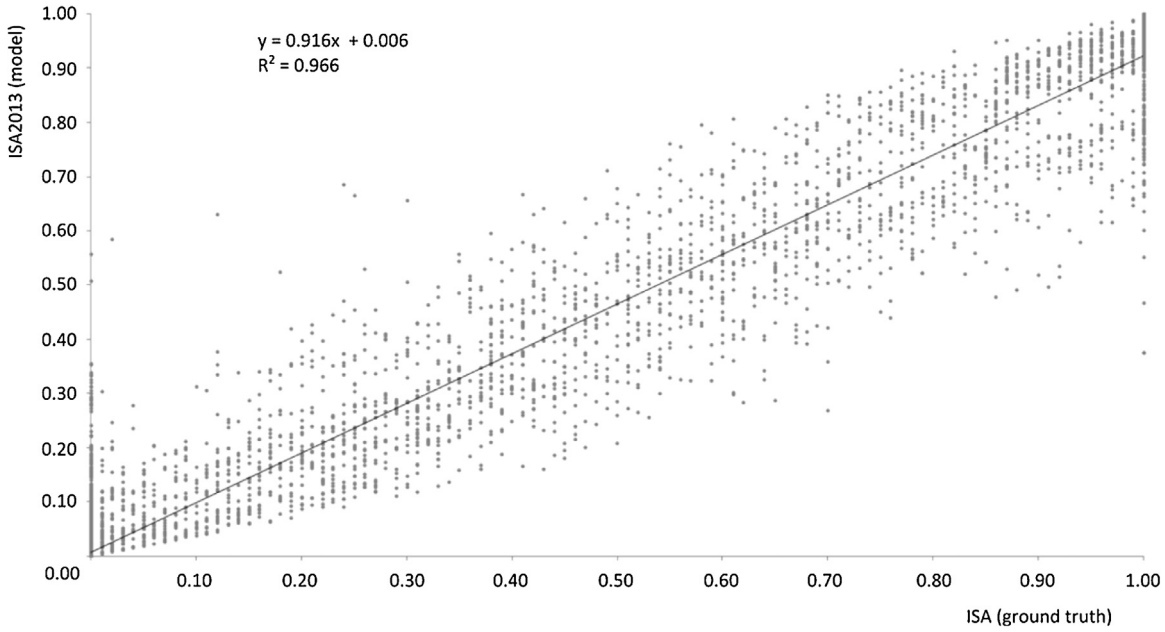

Fig. 4. Correlation of independent ground truth Impervious Surface Area samples and the ISA2013 model.

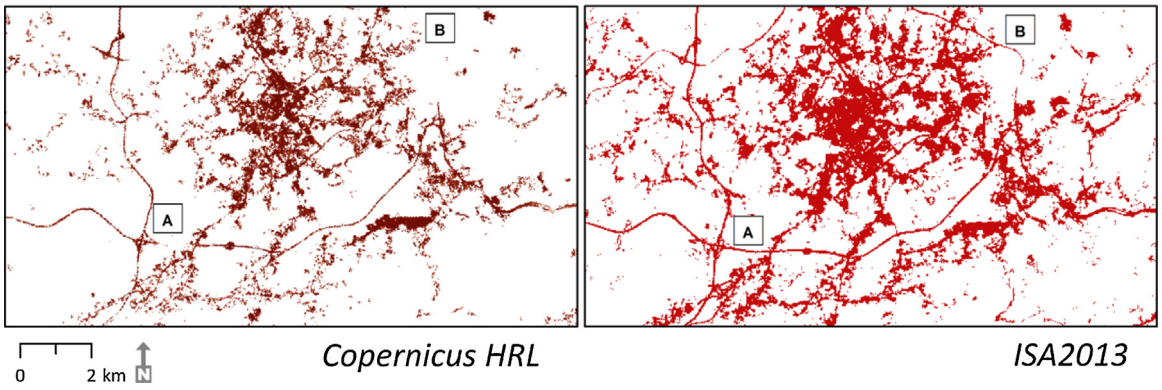

Fig. 5. Comparison of the Copernicus Imperviousness High Resolution Layer and the ISA2013 (depicting pixels with ISA > 10%). A) and B) highlight regions where the ISA is represented erroneously (patchiness) in the Copernicus product in contrast with the more accurate ISA2013 equivalent.

ties (n = 2), parishes (n = 41), and service area rings (i.e. driving times from Coimbra's city center, as described earlier).

Two hypotheses were tested using the ISA time series, including whether 1) the expansion of ISA was correlated with population dynamics and 2) whether the type and intensity of new developments were correlated with initial imperviousness levels.

To evaluate the impact of population change, the parishes were segmented into negative population growth (n = 22) and neutral or positive growth (n = 19) groups. For each parish, the total area of newly developed pixels was calculated for each development class. Finally, single-factor ANOVA was applied to the set, for a significance level of 5%, using Microsoft Excel.

The influence of initial conditions (pre-development, ISA2001) over subsequent ISA (ISA2013) values and development typology (residential, services, and infra-structures) were tested using ANOVA, for a significance level of 5%. This test was followed by Tukey-Kramer's test, both of which were applied at Microsoft Excel. ANOVA was applied to test the equality of means between all groups, after which the Tukey-Kramer test was used to evaluate the pairwise differences between all three development classes. This is adequate as a post-hoc multiple comparison method, which can be applied when the sample sizes are unequal, which was the case in the current application. To this end, the pre-development (ISA2001) and post-development (ISA2013) imperviousness values were extracted for all the changed pixels, which had been manually segmented into the three different development classes.

3. Results

3.1. Impervious surface area 2013 (ISA2013)

The ISA2013 provides basin-wide imperviousness surface fraction estimates at a spatial resolution of 30 m for circa 2013. This model was successfully built for the entire Mondego river Watershed (Fig. 3) and illustrates the different urbanization patterns across the watershed. The ISA2013 map highlights how the densely populated centers of Coimbra and Viseu contrast with the smaller county seats and the forested regions of the Southeast.

The model, based on 148055 training samples (or pixels), included 302 different rules and associated linear regressions, for a predefined minimum of 100 training samples per rule. Several error metrics were calculated to assess the performance of the model. The

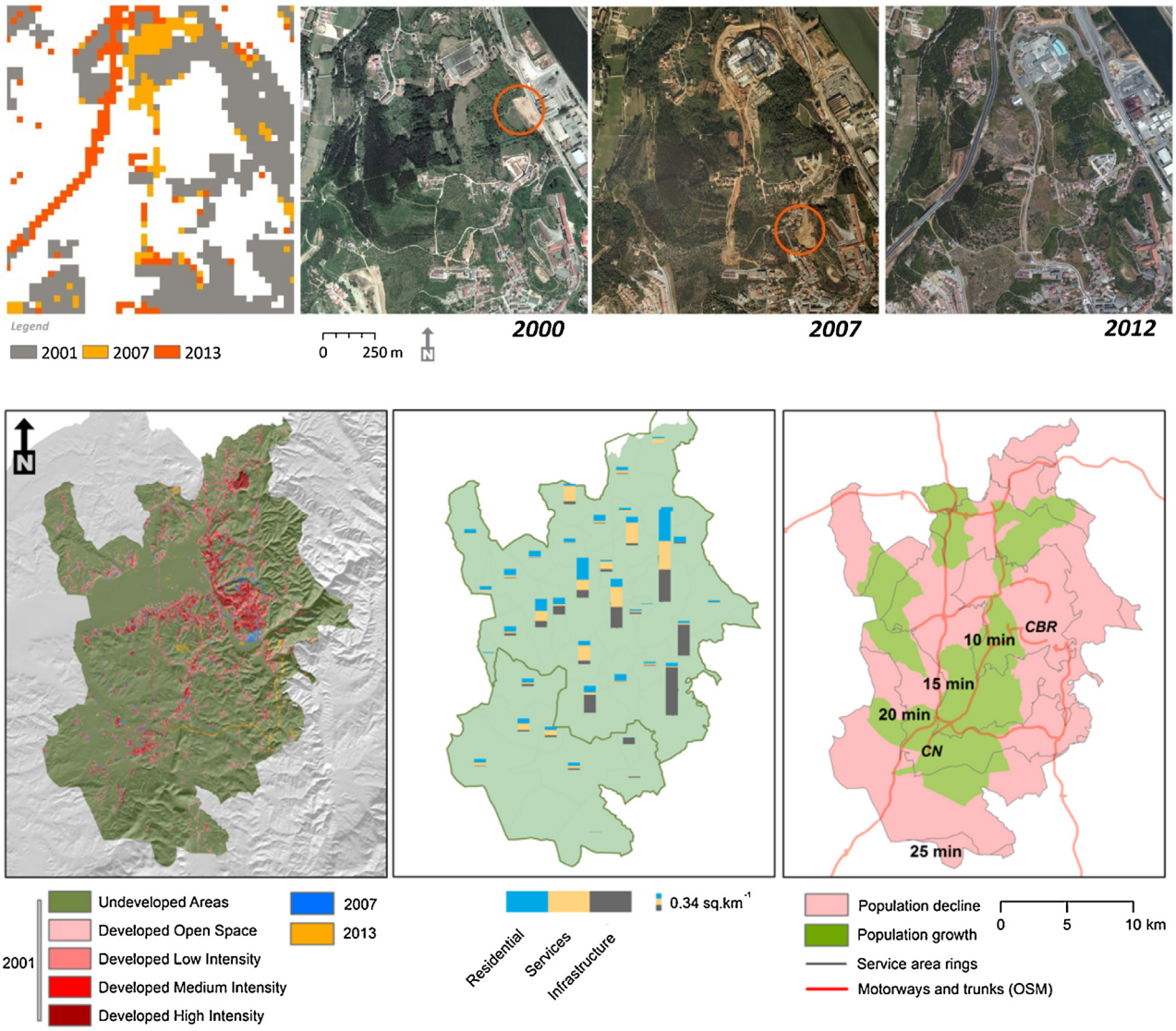

Fig. 6. Top: The models can accurately capture urban change as depicted in the subset. The map shows the evolution of developed land (ISA > 10%) from 2001 to 2013. Transient change (highlighted by the red circles in the aerial images) was accurately recognized as such by the methodology and not classified as impervious surfaces. Bottom: (Left) Imperviousness map showing the development classes (2001) and subsequent developments (2007 and 2013) in the Coimbra and Condeixa-a-Nova counties. (Center) Imperviousness change (2001–2013) characterization into Residential, Services, and Infrastructure categories, per parish. (Right) Population change per parish and service area rings (with traveling times). Motorways and trunks are displayed as well. CN: Condeixa-a-Nova, CBR: Coimbra. (For interpretation of the references to colour in this figure legend, the reader is referred to the web version of this article.)

Correlation Coefficient (r) was of 94.5%. The Mean Absolute Error (MAE) was of 1.6% and the Root-Mean-Square-Error (RMSE) of 5.5%.

The correlation between the ground truth samples (validation subset) and the ISA2013 output is depicted in Fig. 4, which further attests to the good performance of the model.

A derived, categorical map was created from the original ISA2013 with 5 classes: Undeveloped (ISA < 10%), Developed Open Space (DOS) (10% ≤ ISA < 20%), Developed Low Intensity (DLI) (20% ≤ ISA < 50%), Developed Medium Intensity (DMI) (50 ≤ ISA < 80%) and Developed High Intensity (DHI) (ISA > 80%).

The ISA2013 was also visually inspected against the only existing comparable product, the Copernicus Imperviousness High Resolution Layer 2012 (CIHRL). The CIHRL is available as a web service only and no official validation has been published yet.

Fig. 5 compares the imperviousness as estimated by both products for the urban area of Viseu. The CIHRL and the ISA2013 share the common outline of the urban area. Despite the innovative nature of the Copernicus layer, it depicts impervious pixels in a much more discontinuous way, even when ground truth suggests otherwise. In the map, we highlight such situations in A) and B), where the roads are only partially represented or not at all in the CIHRL. The urban center is also depicted in a less realistic manner in the CIHRL, with numerous isolated patches of imperviousness present within the urban matrix. The cumulative impact of these errors is difficult to estimate from a visual interpretation, but may lead to an important underestimation of the imperviousness at the local or regional level.

3.2. Change detection and product updates

Determining a threshold for CVA_{max} was an important step of the product update to earlier dates (2001 and 2007). Two contiguous counties (Coimbra and Condeixa-a-Nova) were selected to test the method. Coimbra is the most populous county in the watershed with 138058 inhabitants in 2013, INE (2015) and is connected to Condeixa-a-Nova (17346 inhabitants in 2013) by numerous routes.

Table 1
Impervious Surface Area fraction (%) statistics (mean and standard deviation) for the two test counties (Coimbra and Condeixa-a-Nova) where the ISA updating strategy was evaluated.

County	2001		2007		2013	
	Mean	SD	Mean	SD	Mean	SD
Coimbra	8.4	19.4	9.1	20.7	11.8	23.5
Condeixa-a-Nova	2.3	9.6	3.1	11.0	4.0	13.1

In fact, the city of Condeixa-a-Nova is the only county seat located within 20 min of Coimbra's city center, under optimum driving conditions, as demonstrated by network analysis at ArcGIS (Fig. 6). Furthermore, the population of Condeixa-a-Nova is increasing, unlike that of Coimbra. It thus offers and interesting comparison of two population centers with a different structure and population dynamics, which might be reflected in the ISA patterns and evolution.

The validation of the CVA-based method suggests that the use of the 2.5% lowest values found within the area (CVA_{max}) is appropriate for the selection of a pool of stable training samples. The overall accuracy of the method is of 94.6% (91.9% Producer's Accuracy and 95.5% User's Accuracy), with a Cohen's Kappa of 0.89. The methodology was thus used to select the suitable pixels for model calibration using 6-year steps (2001 and 2007).

The ISA models were produced after the training samples were screened for change in the subsetted test area using a total of 24158 points for 2013 (extracted from the original pool created for the watershed-wide Research Grade ISA2013), 20997 for 2007, and 18532 for 2001. This means that over the course of 12 years, 76% of the original training samples were still stable, despite the accelerated changes in some areas within the study region. A percentage split of 10% of the sample was chosen to validate the model, using the same error metrics as in the watershed-wide ISA2013.

The ISA2001 had a Pearson Correlation Coefficient (r) of 96.6%, with a MAE of 2.6% and RMSE of 7%. In comparison, the ISA2007 had an r of 95.7%, a MAE of 3.6%, and RMSE of 8%.

The ISA2013 was reprocessed for the purpose of validating the product update strategy using the pool of points located within the subsetted area of interest ($ISA2013_{sub}$) (see Fig. 2 for a description of the workflow). In this instance, the Pearson correlation coefficient was of 96.4%, with a MAE of 2.8% and RMSE of 7.4%. All error metrics show, to some extent, an inferior performance when compared against the 2013 watershed-wide model, possibly as a consequence of the smaller number of ground truth samples used in the calibration.

The production of the 3 models shows the rapid increase of impervious area within the counties (Table 1, Fig. 6). In both cases the change is more abrupt between 2007 and 2013. A simultaneous increase in the diversity of imperviousness fraction values occurred in both counties.

In Coimbra, the average county ISA increased from 8% in 2001 to 9% in 2007, reaching 12% in 2013. From 2001 to 2007, the developed open space and medium intensity ISA classes increased 21.5% and 22.4% respectively. In the period between 2007 and 2013, the fastest growing class is the High Intensity ISA, which increases 51% in comparison with the area estimated for the previous period.

On the other hand, the development in Condeixa-a-Nova is taking place at a faster rate. From 2001 to 2007, developed high intensity pixels increase by 102% and again 101% from 2007 to 2013. The second highest growth rate takes place in Developed Open Space pixels, with an increase of 59% in 2001–2007 and 48% in the later period.

A total of 8944 pixels (or 1.75% of the total area of both counties) were flagged for change and visually inspected. The pixels were characterized in terms of the prevailing function of the newly developed areas, from interpretation of the high resolution imagery and field surveys. Three categories were considered including residential areas (apartment buildings and single-family housing), services (e.g. commercial areas, schools), and infra-structure (e.g. roads, parking lots). Residential areas account for 32.9% of the flagged pixels, Services cover 30.6%, and infrastructure the remainder 36.4% of the total. To determine whether the expansion of impervious areas was driven by population dynamics, the three categories were analyzed for each of the 41 parishes ("Freguesia", the smallest administrative unit of the country) that form the two counties (Fig. 6). The data from the parishes were segmented into positive(and neutral) and negative population change groups as aforementioned. No significant differences were found in all three cases, including for residential areas, after analysis using ANOVA ($p < 0.05$) was applied.

Nonetheless, the starting Imperviousness (ISA2001) in the new developments was found to be different between all categories (ANOVA with a $p < 0.05$, followed by the Tukey-Kramer Test). The lowest initial ISA (before change) was identified in pixels where change was dominated by the construction of new infra-structures mean ISA2001 of 5.4 (standard deviation: 10.3)%. Development for services took place in pixels with an initial ISA (2001) of 9.1 (12.9)% and residential areas in cells with a mean ISA2001 of 11.5 (12.6)%. The final ISA (2013) in flagged pixels was, unlike the starting ISA, different for Residential areas (65.5 (15.9)%) when compared with the other categories, but not between Infra-structure (69.2 (16.6)%) and Services (74.4 (17.6)%) (ANOVA, $p < 0.05$, followed by Tukey-Kramer).

The distance from the center of Coimbra, measured as the optimum driving time (service rings, Fig. 6), offers additional insights regarding the dynamics of urban development. 72.8% of all pixels flagged as changed are found within the two inner rings (0–15 min), even though the ring area accounts for just 45% of the total area of the combined counties. On the other hand, the 20–25 min travel-time ring, which covers 29.6% of the two counties, includes only 4.1% of the pixels flagged for change.

The analysis of ISA2013 patterns within the service area rings, highlights the importance of urban centers in attracting development (Fig. 6). Development in the inner service ring (0–10 min from the city center) is dominated by ISA levels over 20% (DLI: 12.9%, DMI: 12.9%, and DHI: 11.5%), when undeveloped areas (ISA < 10%) are discarded. However, from the second ring onwards, developed pixels are predominantly of the low intensity class (39% of developed pixels), with a decreasing proportion of medium or high intensity ISA2013 (DLI: 6.4%, DMI: 3.4%, and DHI: 1.8%).

3.3. Imperviousness in the watershed

Impervious Surfaces in the Mondego river watershed are distributed in a heterogeneous manner, with local high density areas and vast, mostly unpopulated areas.

With an average ISA2013 of 3.8 (12.3)%, only 8.9% of the pixels in the watershed had an imperviousness fraction greater than 10% and are hence considered as developed. From these, 50.1% were located within 2 km of all motorways and trunks (Fig. 7), even though this buffer covers only 28.6% of the watershed. The coarser CORINE 2012 land cover product, with a spatial resolution of 100 m, points to a much lower estimate of artificial areas (3.3% of the basin, Fig. 1).

The aforementioned development pattern was also perceivable at the sub-basin level. Fig. 7 represents the sub-basins within the Mondego river watershed and highlights the 10% and 30% critical imperviousness levels. 95.4% of the watershed is composed of sub-basins with an average ISA2013 under 10%. However, 4.1% exceeded that threshold and 0.5% were in average more than 30% impervious. The critical areas were mostly coincident with the buffer applied to the main road network. 82.9% of all sub-basins (in

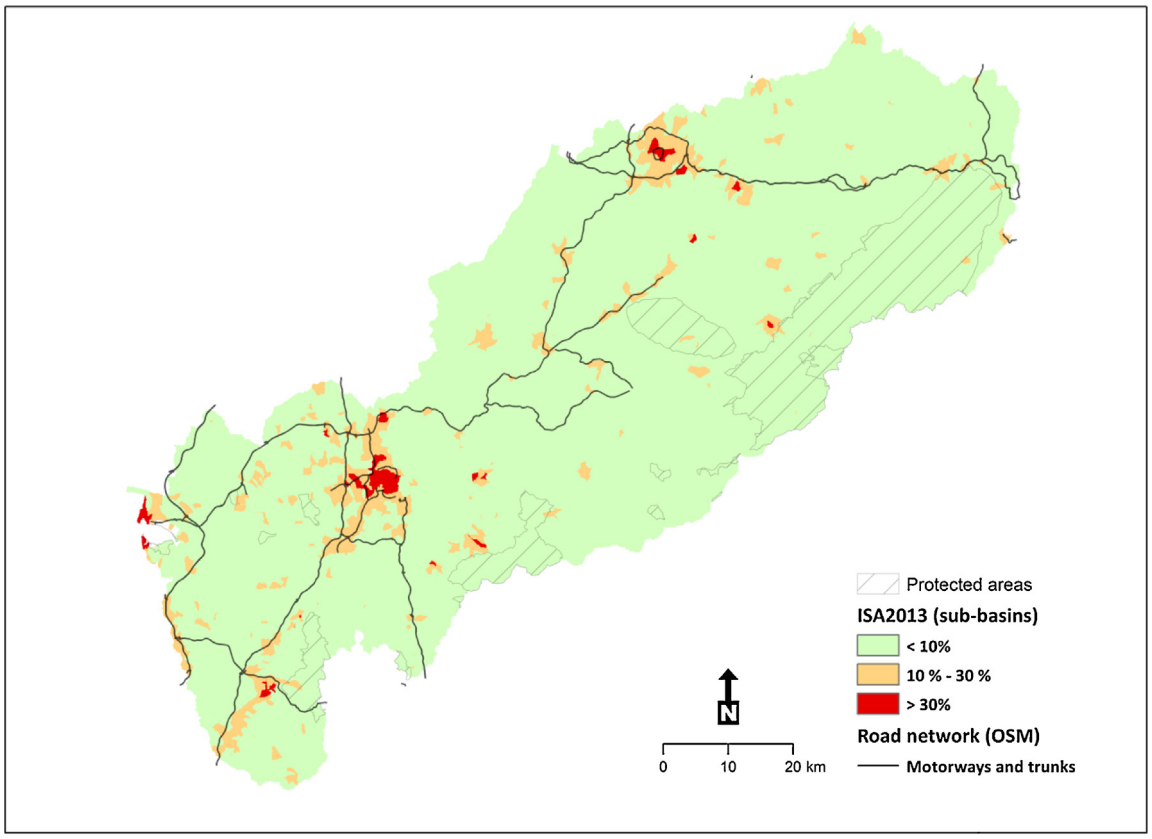

Fig. 7. Catchments within the Mondego river Watershed depicted in function of ISA thresholds (see text for explanation). Protected areas and main road network displayed for reference purposes.

area) with an average ISA2013 greater than 30% were located inside the aforementioned buffer. Similarly, 71.6% of the pixels located in sub-basins where $10\% \leq \text{ISA2013} \leq 30\%$, were found within the buffer.

Several Protected Areas, including natural parks, RAMSAR and Natura 2000 sites are found within the watershed, totaling 893 sq km^{-1} of conservation zones. ISA2013 within these areas was lower than average at 1.2 (5.7) %, reflecting legal and topographic limitations to construction in these regions. Nonetheless, in the vicinity of the parks, within a 5 km buffer, average ISA2013 reached 3.9 (12.8)%. The high imperviousness value (higher than the watershed average) underlines the pressure exerted over some of these important conservation areas.

The census data offers a different perspective on the relation between urbanization and population in the Mondego watershed. The mismatch between the natural and administrative or census boundaries hinders the integration of both components of an otherwise interconnected system.

County population (2013) was compared against ISA2013, when at least 70% of the county was located within the Mondego watershed (and includes the most significant urban center of the county), totaling 24 municipalities. The data suggested that county population and imperviousness were correlated significantly ($r = 0.9$, significant for a $p < 0.01$). Nonetheless, it seems that the correlation is more expressive for counties with a population exceeding 20 000, but the limited number of counties with a population beyond this threshold in the study area (8) precludes further testing of this hypothesis at present.

At the parish level, population density was moderately correlated with ISA2013 ($r = 0.69$, significant for a $p < 0.01$), suggesting other variables influence the spatial distribution of the population at the local level.

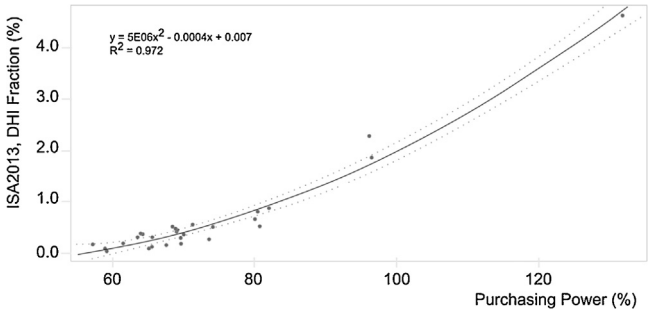

Fig. 8. Purchasing Power of counties as a function of the average Developed High Intensity (DHI) fraction (ISA2013 > 80%) and regression line (solid). Dotted line: 95% Confidence interval.

ISA2013 was also found to be correlated with the purchasing power (PP) (2011) at the county level. However, and even more interestingly, the Developed High Intensity Fraction of ISA (ISA > 80%) was strongly correlated with PP with an r of 0.96 ($p < 0.01$) (Fig. 8).

4. Discussion

4.1. Performance of the methodology

The strategies adopted in this study provide a straightforward and integrated workflow for the production of baseline impervious maps and later updates in a cost-effective way.

Differences in the size, topography, and land cover of the study areas limit the usefulness and reliability of accuracy comparisons with previous studies. Nonetheless, the very low MAE

(ISA2013 = 1.6%), RMSE of 5.5%, and high Correlation Coefficient (r = 94.5%) suggest that the ISA2013 product can be considered research-grade. The overall RMSE of the ISA2013 product was lower than those reported in several works of reference, including Wu (2004) (10.1%) or Xian and Homer (2010), which ranged from 8.5 to 11.15%. The MAE reported by Li et al. (2015) (5.44%) and Esch et al. (2009) (15.0% for the best case) were also higher than the values calculated for the ISA2013. The same applies to the updated prototype maps created for a subset of the watershed.

The comparison against the Copernicus Imperviousness HRL is problematic, since the validation of the product is not yet available. The visual comparison of ISA2013 and CIHRL suggests our product provides a superior representation of the typical connectivity of developed pixels. This advantage of the ISA2013 over the CIHRL is particularly important because it is increasingly relevant to assess not only the prevalence of impervious surfaces (Total impervious Area, TIA) but also the connectivity of these surfaces with the drainage system (Effective Impervious Area, EIA) (Brabec et al., 2002).

Still, the implementation of the mapping workflow was not without challenges. As in previous studies (Bauer et al., 2008; Wu, 2004), tree cover and urban heterogeneity complicated the retrieval of high quality samples and spectral signatures. The use of NDVI time series, with the extraction of the maximum and minimum value of the phenological cycle within a 2σ range, played an essential role in the reduction of uncertainty, namely in cropland and forested areas. Still, densely forested areas (namely in evergreen forests) can obscure impervious surfaces found under the tree canopy and lead to a discontinuity of developed areas that should otherwise be connected in the maps.

The large number of training and validation samples required a long process of delineating polygons and classify them as pervious/impervious. This step, essential for the production of the baseline product, is the most time-consuming step of the processing chain, requiring a trained expert capable of classifying the surfaces from high resolution imagery according to permeability (Yang et al., 2003; Xian, 2008a,b; Jia et al., 2014). The high resolution imagery required to create the training samples that feed the regression tree model may also become a barrier to the adoption of the methodology elsewhere. However, the increasing availability of high resolution imagery may limit this problem, at least for recent reference dates and into the future.

It is important to emphasize that an important aspect of urban imperviousness studies is the ability to compare the estimates for different dates. The methodology presented in this paper, a prototype at this stage, offers a simple, cost-effective way to estimate imperviousness in time series of Landsat data and equivalent sensors. The methodology is based on the selection of stable training samples from the pool of data used in the production of an earlier version. By updating the pool of training samples, and not segments of the baseline products as in previous studies, it is also possible to change the mapping methods, to reflect advances in science and technology. In this study, the proposed method to identify stable samples enabled the production of two updated maps (2001 and 2007) without the production of new samples.

The overall accuracy of the method and the stability of the training samples in the subset of the watershed (76% of the samples were stable during a 12-year period) support its use in this region, as well as in others with similar characteristics. It is also important to emphasize that, despite the stability of the samples, the Coimbra and Condeixa-a-Nova counties were characterized by accelerated LULC changes driven by processes of urban expansion and renewal.

Regardless of the smaller number of training samples used in each update, these products, upon validation, yielded similar accuracies to the original research-grade ISA2013, with a marginal degradation of MAE and RMSE values. The method is thus sufficiently robust for annual updates of ISA maps (at anniversary dates), which seems an adequate periodicity for both scientific studies and management applications. Furthermore, the training sample database can be updated and the model generated shortly after data acquisition, reducing the lag between the reference date and product release. Still, it is important to emphasize that the workflow depends on the availability of compatible data across the entire study period (e.g. Landsat time series).

Ultimately, the seamless updates are only possible because the method is extremely conservative as it excludes all pixels that exceed a very low change magnitude threshold. This is a possible shortcoming, in the sense that it may eliminate a significant number of training samples from land cover classes with naturally high intra and inter-annual variability (e.g. croplands) or disturbed areas with no changes to the anthropogenic imperviousness (e.g. burn scars). On the other hand, it is capable of detecting even small changes to the LULC, as highlighted by the performance metrics. The use of multiple change thresholds (as in Xian et al., 2009) could offer a viable alternative to the presented method, but only when LULC data are available at a common resolution, which is not the case for the study area. The development of additional products, using similar methodologies and spatial resolution, but focusing on other land cover metrics is currently underway and will enable the development of new and improved change detection techniques.

4.2. ISA in the watershed and future work

The Mondego river watershed is characterized by low-to-moderate anthropogenic imperviousness (average ISA of 3.8%), which is distributed asymmetrically across the study area.

Such heterogeneity ensures the existence of vast and mostly undeveloped areas, some of which legally protected but measurably encroached by urbanized regions. ISA values above the watershed average were found in the fringes of the parks and are a cause for concern, as some of these areas are effectively surrounded by nearly-continuous impervious barriers. The ISA product, together with other similar data layers and tools could support the development and enforcement of low-imperviousness corridors in selected, ecologically-significant streams and limit the number of sub-basins exceeding the 10% critical ISA threshold. This is particularly important in a watershed where a significant amount of sub-basins had poor biological or chemical quality (Ferreira et al., 2004) and important areas and water reservoirs are affected by recurrent eutrophication events (Marques et al., 2003; Oliveira and Monteiro, 1992).

Considering the anthropogenic nature of ISA, it is important to combine environmental metrics with the knowledge provided by social, behavioral, and economic sciences (Grimm et al., 2000). This connection is reflected in the increasing demand, by government and managers, of tools capable of quantifying the impact of urban change (Carlson, 2003; Hebble et al., 2001; Young et al., 2013). The resulting information is often on the basis of legislation capable of mitigating the impact of artificialization and internalize the externalities through the taxation of impervious surfaces to promote the protection and restoration of basins (Feitelson and Rotem, 2004; Maryland General Assembly, 2012). Such schemes may leverage an ISA layer such as that suggested in this paper, to implement cost-effective zonal taxation schemes at the sub-basin level, incorporating both objective environmental metrics as well as economic variables at the community level.

In Portugal, several legally binding plans at national, regional and local level exist. These generally set admissible land uses and maximum imperviousness levels and can play a relevant role in the management of urban expansion, as reported for the study area (Monteiro and Tavares, 2015; Tavares et al., 2012). Nonetheless, accurate data on impervious surfaces were not publicly available at

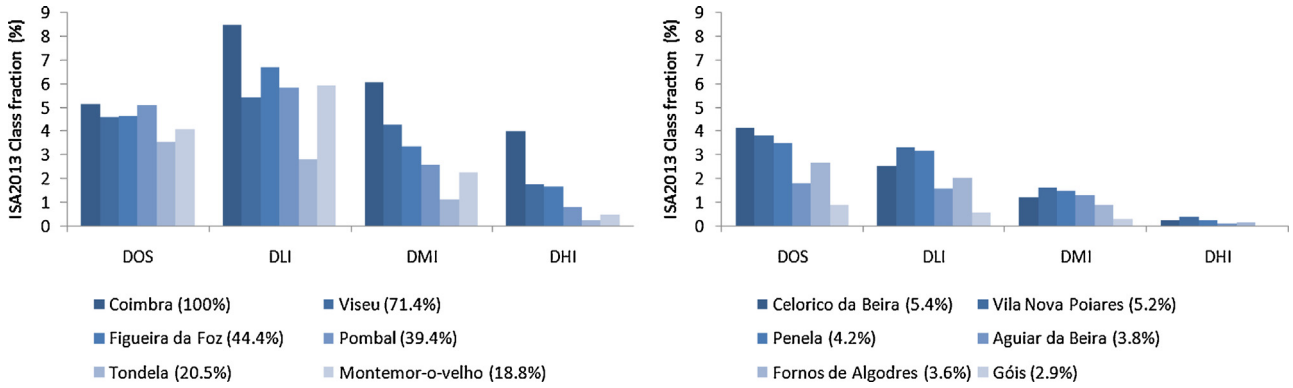

Fig. 9. ISA2013 fraction per development class for the most (left) and less (right) populous counties of the watershed. Population as a percentage of the number of inhabitants of the most populous county (Coimbra) is included in the legend. DOS: Developed Open Space, DLI: Developed Low Intensity, DMI: Developed Medium Intensity, DHI: Developed High Intensity (see text for details).

30 m (or better) resolution and thus a careful and critical scrutiny of urbanization trends was difficult.

Because ISA is the enduring imprint of human activities in a territory, understanding the population dynamics of the watershed is relevant to comprehend the spatial patterns of that variable. Both variables in the watershed mirror the national reality, in which 50% of the population is concentrated in 11% of the counties, predominantly located in coastal regions (INE, 2012). Despite the segmentation of the watershed into 47 counties, approximately 33.2% of the watershed's population resided in Coimbra and Viseu, the largest urban centers of the region, which also account for 20.9% of the total developed pixels in the ISA2013 product.

This dichotomy between developed coastal areas and the depressed hinterland is meaningful from both an ecological and social standpoint. The ISA profiles of the most and least populous counties (Fig. 9) translate the differences in the urban structure, access to services, and infrastructure, which, in the end, influence the livelihood of the communities.

The connection between income structure and land cover processes has been reported to influence – and be influenced by – urban development and imperviousness levels in other regions in similar ways (Hietel et al., 2007; Lu and Weng, 2006). Gross Domestic Product per capita for instance, was demonstrated to be correlated with imperviousness in European cities (Schwarz, 2010; Kraas, 2007). A similar trend seems to be at play in the Mondego Watershed as suggested by the correlation between High Intensity Development (ISA > 80%) and county Purchasing Power (Fig. 8). This was an expected correlation considering the nature of constructions associated to this development class (e.g. highways, dense urban fabric, retail areas, and public venues). The correlation between purchasing power and urban development is in line with findings by Glaeser et al. (2001), which point to quality of life (including access to cultural and commercial spaces) as well as wages as determinant factors capable of ensuring the success of cities.

Nonetheless, shrinkage phenomena affecting cities across Europe (EEA, 2006) may lead to gradual changes in these relations. In fact, the simultaneous acceleration of rural flight phenomena and abandonment of traditional centers, foretell an "everwidening disparity" between different urbanized areas (Glaeser et al., 2001). These changes may also erode the observed correlation between county population and ISA ($r = 0.90$). At the parish level, the population density is already only moderately correlated with ISA ($r = 0.69$) in the Mondego watershed.

The widespread regional population decline is thus only locally reversed as a result of internal rearrangements of the population within the sphere of influence of the main urban centers in a process that was still active after 2001. Relocation to the fringes of the city is often driven by economic and social reasons and perceptions on issues such as the cost of housing or general standards of living (EEA, 2006; McGranahan et al., 2010). However, it is also important to emphasize that these figures already reflect some of the economic, social and population changes caused by the recent sovereign debt crisis, clearly outside the scope of this paper.

A consequence of the complex set of aforementioned mutations, which were recognized in the imperviousness maps produced, is that the new development *loci* become scattered along transportation axes, enabling the daily commute of the new residents towards the traditional economic centers (INE, 2015). It is worth noticing that nearly 73% of pixels flagged for change between 2001 and 2013 in the subsetted study area were located within 15 min of Coimbra's city center. Furthermore, the overwhelming amount of developed pixels in the entire watershed (50.1%) located at a short distance (up to 2 km) of the (asymmetrical) major road network, exemplifies the importance of transportation routes in the construction of ISA spatial patterns in the study area.

Nonetheless, population decline is not always necessarily correlated with ISA dynamics at the temporal scale of the study. Coimbra, despite a significant and persistent population shrinkage between 2001 and 2013 (-10202 inhabitants), witnessed an increase in ISA in the same period. In fact, at the parish level, urban development in Coimbra and Condeixa-a-Nova does not seem to be driven by population changes. Parishes with declining population appear to be as likely to sustain urban growth (including the construction of residential areas) as those with an increasing population. The apparent contradiction can be explained by two different drivers. On the one hand ISA increases are in line with the findings of Panagopoulos and Barreira (2013), which suggest that counties with persistent population decline tend to increase the public expenditure per inhabitant, including in infra-structure. In effect, two thirds of the pixels flagged as changed in the studied counties, comprise either infrastructure or service developments. On the other hand, new residential areas may continue to be constructed as a result of an increase in the per capita use of land as purchasing power improves (Haase et al., 2013), as reported for several emerging counties of the area of study (INE, 2015). Simultaneously, vacant residential buildings are rarely demolished, especially when located in the city center, preventing a reduction of ISA values at the county level.

Interestingly, the starting imperviousness fraction seems to be an important factor driving the type of subsequent development, which could be motivated by land availability and socio-economic factors (Hietel et al., 2007). ISA2001 was lower (5.4%) in pixels where infrastructure was subsequently developed, compared to others where service (9.1%) or residential areas (11.5%) were constructed. The final ISA (2013) of residential areas was, on the other

hand, lower than that of Service or Infrastructure pixels. The natural, cultural, and economic drivers of urban development are clearly at play (Antrop, 2005) and could be monitored and characterized with the ISA product. Determining the location of the development is based on the evaluation of a series of requirements, which differ according to the type of construction. The proximity to existing roads, other dwellings or conversely, the availability of large swaths of undeveloped land influence the initial ISA value per category, which is also characterized by typical final imperviousness levels.

This combination of requirements and characteristics seem to support future attempts to model the sprawl of urban areas in the study area, in response to different scenarios.

The data accuracy and scale as well as the high frequency nature of the methodology thus suggest that specific events, redevelopment projects, and changes to the economic profile of a region can be traced to ISA values while, or shortly after, they take place (e.g. Euro 2004 Soccer Championship or the 'Polis' redevelopment program in Coimbra). Estimating and mapping ISA is thus significant to a broad range of issues in environmental science as well as to characterize the human dimension of this territory. The rapidly evolving landscapes and the spatial scale at which these processes take place call for high temporal resolution of imperviousness products (Weng, 2012) as those enabled by the methodology presented in this paper.

The mapping of the Mondego river Watershed ISA builds on these trends, offering a new, reproducible, and affordable tool to scientists, managers, and decision makers, interested in the local and regional impact of urban development over environmental and socio-economic variables alike.

The development of mapping initiatives focused on watersheds yields information on critical variables for meaningful territories and not just within the often arbitrary and mutable administrative divisions. The geographic consistency of the cartographic products is thus a fundamental aspect of this work, as proposed by previous studies (e.g. Arnold and Gibbons, 1996).

To make the data available to the scientific community and stakeholders, an online platform is currently in development. The project, named 'SmartBasins', is focused on the development of an online cross-platform service where the ISA layers, as well as other geospatial information will be made available in their native and derived formats, with no costs to the users. ISA2013 is the precursor layer to this platform, which aims to address the data needs of a wide range of scientific and operational users. The data thus provided (30-m spatial resolution, with updates every 2 years along with similar retrospective analysis) is in line with identified needs and now a validated protocol enables its operational production (Carlson, 2003; EEA, 2006; Teixeira et al., 2014). A later paper will describe the platform and the different data layers it will provide at the time of launch, supplementing ISA with other critical remotely sensed and modeled metrics.

Additional research will focus on the development of other LULC layers, at a similar or improved spatial resolution and with analogous potential for regular updates. Introducing details into structure and function, analyze connectivity and expand the study of water quality indicators is planned, along with a reinforcement of the classification of agricultural and forested land.

5. Conclusion

At the dawn of the 'age of cities', the momentous challenges ahead call for innovative solutions that combine science, technology and an understating of the social dynamics.

The optimization of urban development policies must be based on sound metrics that spur social and economical development while addressing the needs and hopes of the populations (Marinoni et al., 2013; Duque et al., 2015; Krellenberg et al., 2014).

The ISA2013 was successfully developed and validated to address identified needs not only at a regional level, but Europe-wide. The high accuracy levels of the baseline 2013 product combined with the seamless updating strategy opens new possibilities for the continuous monitoring of an important environmental indicator.

Although the focus of this paper is on the development of ISA mapping methodologies it became clear that the impact of this variable over environmental and social variables deserves further research.

The societal challenges created by a rapidly evolving population structure and changing cultural values are permeating into imperviousness dynamics.

The population is expanding into counties where, traditionally, both population and ISA levels were lower, increasing the pressure over the infrastructure and forcing adjustments, often ad hoc, to the management of the territory. The decentralization of cities will also lead to a multiplication of stressors and the expansion of nonpoint-source pollution as the natural space becomes increasingly fragmented and the soils sealed. The ISA data suggests counties in the study area have thus far failed to adapt to the new reality of declining population, insisting in the expansion of the urbanized surface in an attempt to reverse the shrinkage phenomenon (as also reported by Panagopoulos and Barreira, 2013). The increasingly heavy infrastructure will necessarily have to be maintained by a smaller, older population under a more restrictive budgetary environment.

The development of land use and land cover products that provide reliable and objective metrics was never as relevant as now. Map producers must also consider the appropriate methods and formats for data distribution to guarantee that the data is used by the stakeholders and environmental scientists with no impediments. This has been a central concern of the authors, whom are now developing the SmartBasins platform for ISA (and other) data distribution, integration and modeling. The new opportunities created by the launch of new satellite missions, including ESA's Sentinel constellation, creates interesting perspectives for the future of LULC and the development of sub-pixel, continuous metrics for a better understanding and management of the territory.

Acknowledgements

This study was supported by the FCT (Portuguese Foundation for Science and Technology) through the MARE (Marine and Environmental Sciences Centre) (UID/MAR/04292/2013) Strategic Programme. Vasco Mantas was supported by the PhD FCT grant SFRH/BD/89972/2012.

We are grateful to the anonymous referees for their constructive and insightful comments.

References

Anderson, J.R., Hardy, E.E., Roach, J.T., Witmer, R.E., Peck, D.L., 1976. A Land Use And Land Cover Classification System For Use With Remote Sensor Data, U.S. Geological Survey Circular 671. USGS, Washington, DC.

Andrieu, H., Chocat, B., 2004. Introduction to the special issue on urban hydrology. J. Hydrol. 299, 163–165, http://dx.doi.org/10.1016/j.jhydrol.2004.08.001.

Antrop, M., 2005. Why landscapes of the past are important for the future. Landsc. Urban Plan. 70, 21–34, http://dx.doi.org/10.1016/j.landurbplan.2003.10.002.

Arnold, C.L., Gibbons, C.J., 1996. Impervious surface coverage: the emergence of a key environmental indicator. J. Am. Plan. Assoc. 62, 243–258, http://dx.doi.org/10.1080/01944369608975688.

ARH do Centro IP, 2012. Plano De Gestão Das Bacias Hidrográficas Dos Rios Vouga, Mondego E Lis Integradas Na Região Hidrográfica 4. Ministério daAgricultura, Mar, Ambiente e Ordenamento do Território (accessed May 2015) http://www.apambiente.pt/?ref=16&subref=7&sub2ref=9&sub3ref=834.

Bauer, M.E., Loffelholz, B.C., Wilson, B., 2008. Estimating and maing impervious surface area by regression analysis of landsat imagery. In: Weng, Q. (Ed.), Remote Sensing of Impervious Surfaces. CRC/Taylor & Francis, pp, pp. 3–19.
Bledsoe, B.P., Watson, C.C., 2001. Effects of urbanization on channel instability. J. Am. Water Resour. Assoc. 37, 255–270, http://dx.doi.org/10.1111/j.1752-1688.2001.tb00966.x.
Brabec, E., Schulte, S., Richards, P.L., 2002. Impervious surfaces and water quality: a review of current literature and its implications for watershed planning. J. Plan. Lit. 16, 499–514, http://dx.doi.org/10.1177/088541202400903563.
Breiman, L., Friedman, J.H., Olshen, R.A., Stone, C.J., 1984. Classification and Regression Trees. Wadsworth International Group, Wadsworth Statistics/Probability Serie, Wadsworth.
Cadenasso, M.L., Pickett, S.T.A., Schwarz, K., 2007. Spatial heterogeneity in urban ecosystems: reconceptualizing land cover and a framework for classification. Front. Ecol. Environ. 5, 80–88, http://dx.doi.org/10.1890/1540-9295(2007)5[80:SHIUER]2.0.CO;2.
Carey, R.O., Hochmuth, G.J., Martinez, C.J., Boyer, T.H., Dukes, M.D., Toor, G.S., Cisar, J.L., 2013. Evaluating nutrient impacts in urban watersheds: challenges and research opportunities. Environ. Pollut. 173, 138–149, http://dx.doi.org/10.1016/j.envpol.2012.10.004.
Carlson, T., 2003. Applications of remote sensing to urban problems. Remote Sens. Environ. 86, 273–274, http://dx.doi.org/10.1016/S0034-4257(03)00073-7.
Chadwick, M., Dobberfuhl, D., Benke, A., Huryn, A., Suberkropp, K., Thiele, J., 2006. Urbanization affects stream ecosystem function by altering hydrology, chemistry, and biotic richness. Ecol. Appl. 16 (5), 1796––1807, http://dx.doi.org/10.1890/1051-0761(2006)016[1796:UASEFB]2.0.CO;2.
Chander, G., Huang, C., Yang, L., Homer, C., Larson, C., 2009. Developing consistent landsat data sets for large area applications: the MRLC 2001 protocol. Geosci. Remote Sens. Lett. IEEE 6, 777–781, http://dx.doi.org/10.1109/LGRS.;1;2009.2025244.
Chin, A., 2006. Urban transformation of river landscapes in a global context. Geomorphology 79, 460–487, http://dx.doi.org/10.1016/j.geomorph.2006.06.033.
CORINE, 2016. CORINE Land Cover (last accessed December 2015) http://www.eea.europa.eu/publications/COR0-landcover.
Cunha, P.P., Dinis, J., 2002. In: Pardal, M.A., Marques, J.C., Graça, M.A.S. (Eds.), Sedimentary Dynamics of the Mondego Estuary, In Global Importance of Local Experience—Aquatic Ecology of the Mondego River Basin. Imprensa da Universidade, Coimbra, pp. 43–62 (ISBN: 972-8704-04-6).
Davis, C., Schaub, T., 2005. A transboundary study of urban sprawl in the Pacific Coast region of North America: the benefits of multiple measurement methods. Int. J. Appl. Earth Obs. Geoinf. 7, 268–283, http://dx.doi.org/10.1016/j.jag.2005.06.007.
Deguchi, C., Sugio, S., 1994. Estimations for percentage of impervious area by the use of satellite remote sensing imagery. Water Sci. Technol. 29 (1–2), 135–144.
del Arco, A.I., Verónica, F., Graça, M., 2012. The performance of biological indicators in assessing the ecological state of streams with varying catchment urbanisation levels in Coimbra, Portugal. Limnetica 31, 141–154.
DESTATIS, 2007. Umweltnutzung Und Wirtschaft. Bericht Zu Den Umweltökonomischen Gesamtrechnungen. Statistisches Bundesamt, Wiesbaden (120 p).
Duh, J.-D., Shandas, V., Chang, H., George, L.A., 2008. Rates of urbanisation and the resiliency of air and water quality. Sci. Total Environ. 400, 238–256, http://dx.doi.org/10.1016/j.scitotenv.2008.05.002.
Duque, J.C., Patino, J.E., Ruiz, L.A., Pardo-Pascual, J.E., 2015. Measuring intra-urban poverty using land cover and texture metrics derived from remote sensing data. Landsc. Urban Plan. 135, 11–21, http://dx.doi.org/10.1016/j.landurbplan.2014.11.009.
EEA, 2006. Urban Sprawl in Europe—The Ignored Challenge. European Communities, No 10, Copenhagen, http://dx.doi.org/10.1080/02697451003740312 (60 p).
Emmanuel, R., Krüger, E., 2012. Urban heat island and its impact on climate change resilience in a shrinking city: the case of Glasgow. U. K. Build. Environ. 53, 137–149, http://dx.doi.org/10.1016/j.buildenv.2012.01.020.
Esch, T., Himmler, V., Schorcht, G., Thiel, M., Wehrmann, T., Bachofer, F., Conrad, C., Schmidt, M., Dech, S., 2009. Large-area assessment of impervious surface based on integrated analysis of single-date Landsat-7 images and geospatial vector data. Remote Sens. Environ. 113, 1678–1690, http://dx.doi.org/10.1016/j.rse.2009.03.012.
Feio, M.J., Alves, T., Boavida, M., Medeiros, A., Graça, M.A.S., 2010. Functional indicators of stream health: a river-basin approach. Freshw. Biol. 55, 1050–1065, http://dx.doi.org/10.1111/j.1365-2427.2009.02332.x.
Feitelson, E., Rotem, O., 2004. The case for taxing surface parking. Transp. Res. Part D 9 (4), 319–333 http://dx.doi.org/10.1016/j.trd.2004.04.002.
Ferreira, V., Graça, M., Feio, M.J., Mieiro, C., 2004. Water quality in the Mondego river basin: pollution and habitat heterogeneity. Limnetica 23, 295–306.
Glaeser, E.L., Kolko, J., Saiz, A., 2001. Consumer city. J. Econ. Geogr. 1, 27–50.
Goward, S., Arvidson, T., Williams, D., Faundeen, J., Irons, J., Franks, S., 2006. Historical record of landsat global coverage: mission operations, NSLRSDA, and international cooperator stations. Photogramm. Eng. Remote Sens. 72, 1155–1169.
Grimm, N.B., Grove, J.M., Pickett, S.T.A., Redman, C.L., 2000. Integrated approaches to long-term studies of urban ecological systems. Bioscience 50, 571–584, http://dx.doi.org/10.1641/0006-3568(2000)050.
Groffman, P.M., Bain, D.J., Band, L.E., Belt, K.T., Brush, G.S., Grove, J.M., Pouyat, R.V., Yesilonis, I.C., Zipperer, W.C., 2003. Down by the riverside: urban riparian ecology. Front. Ecol. Environ. 1, 315–321, http://dx.doi.org/10.1890/1540-9295(2003)001[0315:DBTRUR]2.0.CO;2.
Grimm, N., Faeth, S., Golubiewski, N., Redman, C., Wu, J., Bai, X., Briggs, J., 2008. Global change and the ecology of cities. Science 319, 756–760 http://dx.doi.org/10.1126/science.1150195.
Grove, J.M., Burch Jr., W.R., 1997. A social ecology approach and application of urban ecosystem and landscape analysis: a case study of Baltimore Maryland. Urban Ecosyt. 1, 259–275.
Haase, D., Kabisch, N., Haase, A., 2013. Endless urban growth? On the mismatch of population, household and urban land area growth and its effects on the urban debate. PLoS One 8 (6), e66531, http://dx.doi.org/10.1371/journal.pone.0066531.
Hebble, E.E., Carlson, T.N., Daniel, K., 2001. Impervious surface area and residential housing density: a satellite perspective. Geocarto Int. 16, 15–20, http://dx.doi.org/10.1080/10106040108542178.
Herold, M., Gardner, M.E., Roberts, D.A., 2003. Spectral resolution requirements for mapping urban areas. IEEE Trans. Geosci. Remote Sens. 41, 1907–1919, http://dx.doi.org/10.1109/TGRS.2003.815238.
Hietel, E., Waldhardt, R., Otte, A., 2007. Statistical modeling of land-cover changes based on key socio-economic indicators. Ecol. Econ. 62, 496–507, http://dx.doi.org/10.1016/j.ecolecon.2006.07.011.
Hodgson, M.E., Jensen, J.R., Tullis, J.A., Riordan, K.D., Archer, C.M., 2003. Synergistic use of lidar and color aerial photography for mapping urban parcel imperviousness. Photogramm. Eng. Remote Sens. 69 (9), 973–980.
Homer, C., Huang, C., Yang, L., Wylie, B., Coan, M., 2004. Development of a 2001 national land-cover database for the United States. Photogramm. Eng. Remote Sens. 70, 829–840, http://dx.doi.org/10.14358/PERS.70.7.829.
Huang, C., Goward, S.N., Masek, J.G., Thomas, N., Zhu, Z., Vogelmann, J.E., 2010. An automated approach for reconstructing recent forest disturbance history using dense Landsat time series stacks. Remote Sens. Environ. 114, 183–198, http://dx.doi.org/10.1016/j.rse.2009.08.017.
Hurd, J.D., Civco, D.L., 2004. Temporal characterization of impervious surfaces for the State of Connecticut. In: ASPRS Annual Conference Proceedings, Denver, Colorado (Unpaginated CD ROM).
IGP, 2010. Carta De Uso E Ocupação Do Solo De Portugal Continental Para 2007 (COS2007). Memória Descritiva. Instituto Geográfico Português, Lisboa (77 p).
INE, 2012. Censos 2011. Informação à Comunicação Social (in Portuguese). Instituto Nacional de Estatística (Accessed online at www.ine.pt, April 2016, 41 p).
INE, 2014. Projeções de população residente 2012–2060 (in Portuguese). Instituto Nacional de Estatística, Lisbon (March 18 p).
INE, 2015. Digital Census Tables. Instituto Nacional de Estatística (Accessed online at www.ine.pt, May).
Janssen, L.L.F., van der, F.J.M.W., 1994. Accuracy assessment of satellite derived land cover data: a review. Photogramm. Eng. Remote Sens. 60, 419–426.
Jensen, J., Cowen, D., 1999. Remote sensing of urban suburban infrastructure and socio-economic attributes. Photogramm. Eng. Remote Sens. 65, 611–622.
Jia, K., Liang, S., Wei, X., Zhang, L., Yao, Y., Gao, S., 2014. Automatic land-cover update approach integrating iterative training sample selection and a Markov Random Field model. Remote Sens. Lett. 5, 148–156, http://dx.doi.org/10.1080/2150704X.;1;2014.889862.
Jiang, L., Liao, M., Lin, H., Yang, L., 2009. Synergistic use of optical and InSAR data for urban impervious surface mapping: a case study in Hong Kong. Int. J. Remote Sens. 30, 2781–2796, http://dx.doi.org/10.1080/01431160802555838.
Jin, S., Yang, L., Danielson, P., Homer, C., Fry, J., Xian, G., 2013. A comprehensive change detection method for updating the National Land Cover Database to circa 2011. Remote Sens. Environ. 132, 159–175, http://dx.doi.org/10.1016/j.rse.2013.01.012.
Kim, K., Thompson, A.M., Botter, G., 2008. Modeling of thermal runoff response from an asphalt-paved plot in the framework of the mass response functions. Water Resour. Res. 44, 1–13, http://dx.doi.org/10.1029/2007WR005993.
Klein, R.D., 1979. Urbanization and stream quality impairment. Water Resour. Bull. 15 (4), 948–963, http://dx.doi.org/10.1111/j.1752-1688.1979.tb01074.x.
Kraas, F., 2007. Megacities and global change: key priorities. Geogr. J., 79–82.
Krellenberg, K., Link, F., Welz, J., Harris, J., Barth, K., Irarrazaval, F., 2014. Supporting local adaptation: the contribution of socio-environmental fragmentation to urban vulnerability. Appl. Geogr. 55, 61–70, http://dx.doi.org/10.1016/j.apgeog.2014.08.013.
Langanke, T., Büttner, G., Dufourmont, H., Iasillo, D., Probeck, M., Rosengren, Sousa, A., Strobl, P., Weichselbaum, J., 2013. GIO land (GMES/Copernicus initial operations land) High Resolution Layers (HRLs)-summary of product specifications.
Li, M., Zang, S., Wu, C., Deng, Y., 2015. Segmentation-based and rule-based spectral mixture analysis for estimating urban imperviousness. Adv. Sp. Res. 55, 1307–1315, http://dx.doi.org/10.1016/j.asr.;1;2014.12.015.
Loveland, T.R., Sohl, T.L., Stehman, S.V., Gallant, A.L., Sayler, K.L., Napton, D.E., 2002. A strategy for estimating the rates of recent United States land-cover changes. Photogramm. Eng. Remote Sens. 68, 1091–1099.
Lu, D., Weng, Q., 2006. Use of impervious surface in urban land-use classification. Remote Sens. Environ. 102, 146–160 http://dx.doi.org/10.1016/j.rse.2006.02.010.
Macary, F., Morin, S., Probst, J.-L., Saudubray, F., 2014. A multi-scale method to assess pesticide contamination risks in agricultural watersheds. Ecol. Indic. 36, 624–639, http://dx.doi.org/10.1016/j.ecolind.2013.09.001.
Malila, W.A., 1980. Change vector analysis: an approach for detecting forest changes with landsat. In: Proceedings of 6th Annual Symposium on Machine

Processing of Remotely Sensed Data Soil Information Systems and Remote Sensing and Soil Survey, West Lafayette, IN, USA, 3–6 June, pp. 326–335.
Marinoni, O., Higgins, A., Coad, P., Navarro Garcia, J., 2013. Directing urban development to the right places: assessing the impact of urban development on water quality in an estuarine environment. Landsc. Urban Plan. 113, 62–77, http://dx.doi.org/10.1016/j.landurbplan.2013.01.010.
Marques, J.C., Graça, M.A., Pardal, M.A., 2002. Introducing the Mondego river basin. In: Pardal, M.A., Marques, J.C., Graça, M.A.S. (Eds.), Global Importance of Local Experience—Aquatic Ecology of the Mondego River Basin. Imprensa da Universidade, Coimbra, pp. 7–12 (ISBN: 972-8704-04-6).
Marques, J.C., Nielsen, S.N., Pardal, M.A., Jørgensen, S.E., 2003. Impact of eutrophication and river management within a framework of ecosystem theories. Ecol. Model 166, 147–168, http://dx.doi.org/10.1016/S0304-3800(03)00134-0.
Marques, J.C., Basset, A., Brey, T., Elliott, M., 2009. The ecological sustainability trigon—a proposed conceptual framework for creating and testing management scenarios. Mar. Pollut. Bull. 58, 1773–1779, http://dx.doi.org/10.1016/j.marpolbul.2009.08.020.
Martínez-Fernández, J., Ruiz-Benito, P., Zavala, M.a., 2015. Recent land cover changes in Spain across biogeographical regions and protection levels: implications for conservation policies. Land Use Policy 44, 62–75, http://dx.doi.org/10.1016/j.landusepol.2014.11.021.
Maryland General Assembly, 2012. House Bill 987, Stormwater Management − Watershed Protection and Restoration Program.
Masek, J.G., Vermote, E.F., Saleous, N., Wolfe, R., Hall, F.G., Huemmrich, F., Gao, F., Kutler, J., Lim, T.K., 2013. LEDAPS Calibration, Reflectance, Atmospheric Correction Preprocessing Code, Version 2. Model product. Oak Ridge National Laboratory Distributed Active Archive Center, Oak Ridge, Tennessee, U.S.A, http://dx.doi.org/10.3334/ORNLDAAC/1146, Available on-line [http://daac.ornl.gov].
McClure, C.J.W., Korte, A.C., Heath, J.A., Barber, J.R., 2015. Pavement and riparian forest shape the bird community along an urban river corridor. Glob. Ecol. Conserv. 4, 291–310, http://dx.doi.org/10.1016/j.gecco.2015.07.004.
McGranahan, D., Cromartie, J., Wojan, T., 2010. Nonmetropolitan Outmigration Counties: Some Are Poor, Many Are Prosperous. United States Department of Agriculture (USDA), Economic Research Service, ERR-107 (29 pp).
Miltner, R., White, D., Yoder, C., 2004. The biotic integrity of streams in urban and suburbanizing landscapes. Landsc. Urban Plan. 69 (1), 87–100, http://dx.doi.org/10.1016/j.landurbplan.2003.10.032.
Monteiro, M., Tavares, A.O., 2015. What is the influence of the planning framework on the land use change trajectories? Photointerpretation analysis in the 1958–2011 period for a medium/small sized city. Sustainability 7, 11727–11755, http://dx.doi.org/10.3390/su70911727.
Morisawa Marie, Ernest LaFlure, 1979. Hydraulic geometry, stream equilibrium and urbanization. In: Rhodes, D.D., Williams, G.P. (Eds.), Adjustments of the Fluvial Systems—Proceedings of the 10th Annual Geomorphology Symposium Series. Binghamton, NY.
OSM, (last accesses January 2015) http://www.openstreetmap.org.
Oliveira, M.R.L., Monteiro, M.T., 1992. Blooms De Cyanophyceae Na Albufeira Da Aguieira: Efeitos Na Qualidade Da água E No Zooplâncton, vol. 61. Relatório Técnico Científico INIP (57p.).
Pacifici, F., 2014. The importance of physical quantities for the analysis of multitemporal and multiangular optical very high spatial resolution Images. IEEE Trans. Geosci. Remote Sens. 52 (10), 6241–6256.
Panagopoulos, T., Barreira, A.P., 2013. Understanding the shrinkage phenomenon in Portugal. WSEAS Trans. Environ. Dev. 9, 1–12.
Parece, T.E., Campbell, J.B., 2013. Comparing urban impervious surface identification using Landsat and high resolution aerial photography. Remote Sens. 5, 4942–4960, http://dx.doi.org/10.3390/rs5104942.
Paul, M., Meyer, J., Couch, C., 2006. Leaf breakdown in streams differing in catchment land use. Freshw. Biol. 51 (9), 1684–1695, http://dx.doi.org/10.1111/j.1365-2427.2006.01612.x.
Pickett, S.T. a., Cadenasso, M.L., Grove, J.M., Groffman, P.M., Band, L.E., Boone, C.G., Burch, W.R., Grimmond, C.S.B., Hom, J., Jenkins, J.C., Law, N.L., Nilon, C.H., Pouyat, R.V., Szlavecz, K., Warren, P.S., Wilson, M. a., 2008. Beyond urban legends: an emerging framework of urban ecology, as illustrated by the Baltimore ecosystem study. Bioscience 58, 139, http://dx.doi.org/10.1641/B580208.
Pilli, R., 2012. Calibrating CORINE land cover 2000 on forest inventories and climatic data: an example for Italy. Int. J. Appl. Earth Obs. Geoinf. 19, 59–71, http://dx.doi.org/10.1016/j.jag.2012.04.016.
Quinlan, J.R., 1992. Learning with Continuous Classes. In: 5th Australian Joint Conference on Artificial Intelligence. World Scientific, Singapore, pp. 343–348.
Raciti, S.M., Hutyra, L.R., Newell, J.D., 2014. Mapping carbon storage in urban trees with multi-source remote sensing data: relationships between biomass, land use, and demographics in Boston neighborhoods. Sci. Total Environ. 500–501, 72–83, http://dx.doi.org/10.1016/j.scitotenv.2014.08.070.
Ridd, M.K., 1995. Exploring a V-I-S (vegetation-impervious surface-soil) model for urban ecosystem analysis through remote sensing: comparative anatomy for cities. Int. J. Remote Sens. 16, 2165–2185, http://dx.doi.org/10.1080/01431169508954549.
Roy, A.H., Rosemond, A.D., Paul, M.J., Leigh, D.S., Wallace, J.B., 2003. Stream macroinvertebrate response to catchment urbanisation (Georgia, USA). Freshw. Biol. 48 (2), 329–346, http://dx.doi.org/10.1046/j.1365-2427.2003.00979.x.
Schwarz, N., 2010. Urban form revisited—selecting indicators for characterising European cities. Landsc. Urban Plan. 96, 29–47, http://dx.doi.org/10.1016/j.landurbplan.2010.01.007.
Sexton, J.O., Song, X.P., Huang, C., Channan, S., Baker, M.E., Townshend, J.R., 2013. Urban growth of the Washington, D.C.-Baltimore, MD metropolitan region from 1984 to 2010 by annual, Landsat-based estimates of impervious cover. Remote Sens. Environ. 129, 42–53, http://dx.doi.org/10.1016/j.rse.2012.10.025.
Slonecker, E.T., Jennings, D.B., Garofalo, D., 2001. Remote sensing of impervious surfaces: a review. Remote Sens. Rev. 20, 227–255, http://dx.doi.org/10.1080/02757250109532436.
Song, Y., Li, F., Wang, X., Xu, C., Zhang, J., Liu, X., Zhang, H., 2015. The effects of urban impervious surfaces on eco-physiological characteristics of Ginkgo biloba: a case study from Beijing, China. Urban For. Urban Green. 14 (4), 1102–1109, http://dx.doi.org/10.1016/j.ufug.2015.10.008.
Stathopoulou, M., Cartalis, C., 2007. Daytime urban heat islands from Landsat ETM+ and CORINE land cover data: an application to major cities in Greece. Sol. Energy 81, 358–368, http://dx.doi.org/10.1016/j.solener.2006.06.014.
Suau-Sanchez, P., Burghouwt, G., Pallares-Barbera, M., 2014. An appraisal of the CORINE land cover database in airport catchment area analysis using a GIS approach. J. Air Transp. Manage. 34, 12–16, http://dx.doi.org/10.1016/j.jairtraman.2013.07.004.
Tavares, A.O., Pato, R.L., Magalhães, M.C., 2012. Spatial and temporal land use change and occupation over the last half century in a peri-urban area. Appl. Geogr. 34, 432–444, http://dx.doi.org/10.1016/j.apgeog.2012.01.009.
Teixeira, Z., Teixeira, H., Marques, J.C., 2014. Systematic processes of land use/land cover change to identify relevant driving forces: implications on water quality. Sci. Total Environ. 470–471, 1320–1335, http://dx.doi.org/10.1016/j.scitotenv.2013.10.098.
Thomas, N., Hendrix, C., Congalton, R.G., 2003. A comparison of urban mapping methods using high-resolution digital imagery. Photogramm. Eng. Remote Sens. 69 (9), 963–972, http://dx.doi.org/10.14358/PERS.69.9.963.
Tiner, R.W., 2004. Remotely-sensed indicators for monitoring the general condition of natural habitat in watersheds: an application for Delaware's Nanticoke River watershed. Ecol. Indic. 4, 227–243, http://dx.doi.org/10.1016/j.ecolind.2004.04.002.
Turner, B.L., Lambin, E.F., Reenberg, A., 2007. The emergence of land change science for global environmental change and sustainability. Proc. Natl. Acad. Sci. U. S. A. 104, 20666–20671, http://dx.doi.org/10.1073/pnas.0704119104.
U.N, 2014. World Urbanization Prospects, the 2014 Revision (ST/ESA/SER.A/352). United Nations, Department of Economic and Social Affairs, Population Division, New York, http://dx.doi.org/10.4054/DemRes.2005.12.9 (27 p.).
U.S. Department of Agriculture, 2013. Summary Report: 2010 National Resources Inventory. Natural Resources Conservation Service and Center for Survey Statistics and Methodology, Iowa State University, Washington, DC.
United States Geological Survey, 2015. Provisional Landsat 8 Surface Reflectance Product. Product Guide.Version 1.3. Department of the Interior, United States Geological Survey (27 p. http://landsat.usgs.gov/documents/provisional_l8sr_product_guide.pdf, accessed May 2015).
Van der Linden, S., Hostert, P., 2009. The influence of urban structures on impervious surface maps from airborne hyperspectral data. Remote Sens. Environ. 113, 2298–2305, http://dx.doi.org/10.1016/j.rse.2009.06.004.
Veach, A.M., Bernot, M.J., 2011. Temporal variation of pharmaceuticals in an urban and agriculturally influenced stream. Sci. Total Environ. 409, 4553–4563, http://dx.doi.org/10.1016/j.scitotenv.2011.07.022.
Vietz, G.J., Sammonds, M.J., Walsh, C.J., Fletcher, T.D., Rutherfurd, I.D., Stewardson, M.J., 2014. Ecologically relevant geomorphic attributes of streams are impaired by even low levels of watershed effective imperviousness. Geomorphology 206, 67–78, http://dx.doi.org/10.1016/j.geomorph.2013.09.019.
Walsh, C.J., Roy, A.H., Feminella, J.W., Cottingham, P.D., Groffman, P.M., Morgan, R.P., 2005. The urban stream syndrome: current knowledge and the search for a cure. J. N. Am. Benthol. Soc. 24, 706–723, http://dx.doi.org/10.1899/04-028.1.
Weng, Q., 2001. Modeling urban growth effects on surface runoff with the integration of remote sensing and GIS. Environ. Manage. 28, 737–748, http://dx.doi.org/10.1007/s002670010258.
Weng, Q., 2012. Remote sensing of impervious surfaces in the urban areas: requirements, methods, and trends. Remote Sens. Environ. 117, 34–49, http://dx.doi.org/10.1016/j.rse.2011.02.030.
White, M., Grier, K., 2006. The effects of watershed urbanization on the stream hydrology and riparian vegetation of los peñasquitos creek, california. Landsc. Urban Plan. 74, 125–138, http://dx.doi.org/10.1016/j.landurbplan.2004.11.015.
Wu, C., 2004. Normalized spectral mixture analysis for monitoring urban composition using ETM+ imagery. Remote Sens. Environ. 93, 480–492, http://dx.doi.org/10.1016/j.rse.2004.08.003.
Xian, G., 2008a. Mapping impervious surfaces using classification and regression tree algorithm. In: Weng, Q. (Ed.), Remote Sensing of Impervious Surfaces. CRC/Taylor & Francis, pp. 39–58.
Xian, G., 2008b. Satellite remotely-sensed land surface parameters and their climatic effects for three metropolitan regions. Adv. Space Res. 41, 1861–1869, http://dx.doi.org/10.1016/j.asr.2007.11.004.
Xian, G., Homer, C., Fry, J., 2009. Updating the 2001 National Land Cover Database land cover classification to 2006 by using Landsat imagery change detection methods. Remote Sens. Environ. 113, 1133–1147, http://dx.doi.org/10.1016/j.rse.2009.02.004.
Xian, G., Homer, C., 2010. Updating the 2001 national land cover database impervious surface products to 2006 using landsat imagery change detection

methods. Remote Sens. Environ. 114, 1676–1686, http://dx.doi.org/10.1016/j.rse.2010.02.018.
Yang, L., Xian, G., Klaver, J.M., Deal, B., 2003. Urban land-cover change detection through sub-pixel imperviousness mapping using remotely sensed data. Photogramm. Eng. Remote Sens. 69, 1003–1010, http://dx.doi.org/10.14358/PERS.69.9.1003.
Young, D., Afoa, E., Meijer, K., Wagenhoff, A., Utech, C., 2013. Temperature as a contaminant in streams in the Auckland region, stormwater issues and management options. Prepared by Morphum Environmental Ltd for Auckland Council Auckland Council Technical Report, TR2013/044.
Yuan, F., Bauer, M.E., 2007. Comparison of impervious surface area and normalized difference vegetation index as indicators of surface urban heat island effects in Landsat imagery. Remote Sens. Environ. 106, 375–386, http://dx.doi.org/10.1016/j.rse.2006.09.003.
Yuan, F., Wu, C., Bauer, M.E., 2008. Comparison of spectral analysis techniques for impervious surface estimation using landsat imagery. Photogramm. Eng. Remote Sens. 74 (8), 1045–1055.
Zhang, H., Zhang, Y., Lin, H., 2012. A comparison study of impervious surfaces estimation using optical and SAR remote sensing images. Int. J. Appl. Earth Obs. Geoinf. 18, 148–156, http://dx.doi.org/10.1016/j.jag.2011.12.015.
Zhang, J., He, C., Zhou, Y., Zhu, S., Shuai, G., 2014a. Prior-knowledge-based spectral mixture analysis for impervious surface mapping. Int. J. Appl. Earth Obs. Geoinf. 28, 201–210, http://dx.doi.org/10.1016/j.jag.2013.12.001.
Zhang, J., Li, P., Wang, J., 2014b. Urban built-up area extraction from landsat TM/ETM+ images using spectral information and multivariate texture. Remote Sens. 6, 7339–7359, http://dx.doi.org/10.3390/rs6087339.
Zhang, Y., Zhang, H., Lin, H., 2014c. Improving the impervious surface estimation with combined use of optical and SAR remote sensing images. Remote Sens. Environ. 141, 155–167, http://dx.doi.org/10.1016/j.rse.2013.10.028.